4. Quantum Many-Body Problems

D. M. Ceperley and M. H. Kalos

With 4 Figures

Abstract

We review methods used and results obtained in Monte Carlo calculations on quantum fluids and crystals. Available techniques are discussed for the computation of the energy and other expectation values by variational methods in which the absolute square of a trial function ψ_T is sampled by the Metropolis method. Recently developed methods for fermion systems are included. We give a more detailed exposition of the Green's Function Monte Carlo method which permits exact numerical estimates of boson ground-state properties. Our survey of results comprises applications to ^{3}He and ^{4}He, hard-sphere fluids and crystals, spin-aligned hydrogen, the one-component plasma for bosons and fermions, and simple models of neutron and nuclear matter. The reliability of the product form of ψ_T in several applications is assessed. A selected set of related topics is also taken up: low temperature excitations, results obtained by the Wigner $\hbar$ expansion, and evaluations of virial coefficients and pair correlations at finite temperatures.

In this chapter, we give a survey of the applications of Monte Carlo methods to the study of quantum phenomena in statistical physics. The emphasis is on the modelling of many-particle systems which exhibit quantum effects at the macroscopic level - systems such as liquids and crystals of helium and the electron gas. Such work is complementary to a vast literature in which more tranditional theoretical methods have been applied to these systems. Space precludes citing more than the most striking and significant treatments of that kind.

$\hbar = h/2\pi$ (normalized Planck's constant)

4.1 Introductory Remarks

Monte Carlo simulation of quantum many-body systems dates from McMILLAN's observation [4.1] that for a trial wave function having the form of a product of two-body correlation factors, the integrals required to evaluate expectations — including the total energy — can be carried out by the method of METROPOLIS et al. (cf. Chap.1 and Sect.4.2.1 below). The overwhelming bulk of research has been carried out on this basis. We describe in Sect.4.2 the range of direct applications of McMILLAN's method to a variety of physical systems as well as some extensions of the basic idea. We shall see that these simulations have been fruitful, providing useful results and insight into both physical processes and the structure of successful theories. In some cases, associated with hard-core potentials, however, product trial wave functions omit certain important properties of the ground state and the variational estimates are not accurate enough for quantitative comparison with experiment. This is true, for example, for the ground state of ^{4}He where the variational estimates of energy are 15-20% too high, precluding critical comparison of different force laws.

A more powerful — but more elaborate — method has been developed which permits in principle the Monte Carlo solution of the Schrödinger equation. It has come to be called the Green's Function Monte Carlo (GFMC) and in Sect.4.4 we will describe its general principles, its practical problems, and the results which have been obtained with its use.

Some special topics will also be discussed much more briefly: quantum corrections to classical simulations of light atoms, systems with low temperature excitations, and calculations of quantum virial coefficients.

Simulations of quantum spin lattices [4.2,3] will not be discussed as they have not yet produced many very useful results, although they are potentially interesting.

4.2 Variational Methods

The variational method has proved to be a very useful way of computing ground-state properties of many-body systems. Conceptually it is quite simple. The variational principle tells us that for any function $\psi_T(\underline{R})$, the variational energy E_T, defined as

$$E_T = \int d\underline{R}\ \psi_T(\underline{R})H(\underline{R})\psi_T(\underline{R}) / \int d\underline{R}|\psi_T(\underline{R})|^2 \qquad (4.1)$$

will be a minimum when ψ_T is the ground-state solution of the Schrödinger equation (here $\underline{R}$ refers to the coordinates of the N particles), and $H(\underline{R})$ is the hamiltonian. The trial function of course must be either symmetric or antisymmetric with respect to the coordinates depending on the statistics of the particles. The variational method then consists of constructing a family of functions $\psi_T(\underline{R},\underline{a})$ and optimizing the parameters $\underline{a}$ so that the energy (4.1) is minimized for $\underline{a} = \underline{a}^*$. The variational energy is a rigorous upper bound to the ground-state energy and if the family of functions was chosen well, $\psi_T(\underline{R},\underline{a}^*)$ will be a good approximation to the ground-state wave function.

The problem of constructing a good trial function for a Bose liquid at zero temperature seems to have been considered first by BIJL [4.4]. Consider a liquid of hard spheres; we shall see later that this is a good model for liquid helium. The wave function clearly must vanish if any pair of particles overlaps. The simplest way to satisfy these conditions is to make the trial function a product of two-particle correlation functions, $f(|\underline{r}_i - \underline{r}_j|)$. That is the BIJL wave function

$$\psi_T = \prod_{i<j} f(r_{ij}) \equiv \exp\left[-\frac{1}{2}\sum_{i<j} u(r_{ij})\right] \quad . \tag{4.2}$$

The "pseudopotential" $u(r)$ for an isotropic liquid is a function of the radial separation only. The square of this trial function is completely equivalent to the Boltzmann distribution of a classical system with $u(r)$ replaced by the interatomic potentials over kT (hence the name "pseudopoential"). BIJL showed how ψ_T arises naturally from perturbation theory at low densities, and with a proper choice of $u(r)$, ψ_T will have many of the correct macroscopic properties.

This form was reinvented by DINGLE [4.5], JASTROW [4.6] and MOTT [4.7] and generalized for Fermi liquids

$$\psi_T = D(\underline{R}) \exp\left[-\frac{1}{2}\sum_{i<j} u(r_{ij})\right] \tag{4.3}$$

where $D(\underline{R})$ is the ideal Fermi gas wave function, i.e., a determinant of plane waves. The form of the product trial function in a quantum crystal was considered by SAUNDERS [4.8]. His form of the trial function is

$$\psi_T(\underline{R}) = \exp\left[-\frac{1}{2}\sum_{i<j} u(r_{ij})\right] \sum_P (\pm 1)^P \phi(\underline{r}_i - s_{P_i}) \eta_{\sigma_i \sigma_{P_i}} \tag{4.4}$$

where $\phi(\underline{r})$ is a single-particle orbital about a lattice site, usually taken to be a Gaussian function, P is a permutation of the pairing of particles to lattice

sites, $\underline{s}$; η is a spinor, and the $\pm$ signs are for Bose or Fermi statistics, respectively.

The pseudopotential u(r) in these equations, in contrast to the classical situation, is varied to minimize the energy in (4.1). In practice, the pseudopotential is chosen to have some functional form with several free parameters which are then varied. For a hard-sphere system u must be infinitely repulsive for r less than the hard-sphere diameter. For the optimum pseudopotential it is easy to show that the variational energy when two particles are constrained to be a fixed distance, r, apart, $E_v(r)$, is independent of r and equal to the unconstrained variational energy in (4.1). If the interparticle potential is singular at the origin then one can determine the small r behavior of the optimum pseudopotential by requiring that $E_v(r)$ be finite as two particles approach each other. This leads to the condition

$$\lim_{r\to 0}\left\{ v(r) + \frac{\hbar^2}{2m}\left[\nabla^2 u(r) - \frac{1}{2}\left(\frac{du}{dr}\right)^2 + \delta_{\sigma_i\sigma_j}\frac{2}{r}\frac{du}{dr}\right]\right\} = \text{constant} + O\left(\frac{\hbar^2}{2m} r \frac{du}{dr}\right) \tag{4.5}$$

where v(r) is the interparticle potential and σ_i and σ_j are the spin coordinates. The "spin coordinates" are in effect always different for bosons since there is no Slater determinant in their trial function. For fermions the optimum u(r) will depend on the relative spin coordinates.

The large behavior of u(r) can be derived from essentially macroscopic arguments or with the random phase approximations by demanding that the energy not change if there are long wavelength density oscillations present. For short-range interparticle potentials (i.e., not Coulomb), the macroscopic argument gives that

$$u(r) \cong \frac{mc}{\rho\pi^2\hbar r^2} \quad . \tag{4.6}$$

REATTO and CHESTER [4.9] have shown that this pseudopotential will give the correct linear behavior for small k in S(k) which is believed to be necessary [4.10] for superfluiditiy. KROTSCHECK [4.11] has shown that for the optimum u, c is an upper bound to the speed of sound in the exact ground state. For a repulsive Coulomb system, as is well known, the structure function is proportional to k^2 at small k because of the plasma modes, independent of particle statistics or temperature. BOHM [4.12] has shown that this implies the following large-r behavior of the pseudopotential

$$u(r) \cong Z \frac{e}{\hbar} \sqrt{\frac{m}{\pi\rho}} \frac{1}{r} \quad . \tag{4.7}$$

We have given some reasons for believing that the use of the product trial function can be a good approximation for quantum systems. The task now is to evaluate the multidimensional integrals to get expectation values, in particular to calculate the variational energy for (4.1). There have been many approaches to this problem, practically all of them borrowed from the theory of classical fluids: namely cluster expansions, integral equations, the Metropolis Monte Carlo method, and even molecular dynamics. The Monte Carlo algorithm [of METROPOLIS, A. ROSENBLUTH, M. ROSENBLUTH, A. TELLER, and E. TELLER [4.13] or $M(RT)^2$] is particularly well suited to this problem of calculating multidimensional integrals and has the distinct advantage over the approximate expansions that there are no approximations made that cannot be tested within the method. Molecular dynamics has been successfully applied to Bose liquids but almost all results have been obtained using Monte Carlo.

We will now describe the $M(RT)^2$ Monte Carlo algorithm for sampling the product trial function and in some detail show how it is used to find ground state properties. Then we will describe some of the many calculations that have been made with this algorithm and what has been learned from the variational studies.

4.2.1 Monte Carlo Methods with the Product Trial Function

The Monte Carlo algorithm $M(RT)^2$ [4.13] which was invented to calculate properties of classical statistical systems, is an extremely powerful way to compute multidimensional integrals. For quantum systems we want an algorithm which will produce configurations with a probability proportional to the square of the wave function. Any measurable quantity can be written as an average over such configurations. Suppose A is an operator and we wish to compute its expectation value defined as

$$\langle A \rangle = \frac{\int d\underline{R}\, \psi_T^*(\underline{R})\, A\, \psi_T(\underline{R})}{\int d\underline{R} |\psi_T(\underline{R})|^2} \quad . \tag{4.8}$$

Let $\{\underline{R}_i\}$ be a set of points drawn from the probability distribution

$$p(\underline{R}) = \frac{|\psi_T(\underline{R})|^2}{\int |\psi_T(\underline{R})|^2 d\underline{R}} \tag{4.9}$$

where the integral in the denominator serves here merely to normalize $p(\underline{R})$. Then

for any function $f(\underline{R})$, the central limit theorem of probability gives that

$$\lim_{M\to\infty} \frac{1}{M} \sum_{i=1}^{M} f(\underline{R}_i) = \frac{\int f(\underline{R})|\psi_T(\underline{R})|^2 d\underline{R}}{\int |\psi_T(\underline{R})|^2 d\underline{R}} \tag{4.10}$$

and in particular

$$\lim_{M\to\infty} \frac{1}{M} \sum \psi_T^{-1}(\underline{R}_i) A(\underline{R}) \psi_T(\underline{R}_i) = \langle A \rangle \quad . \tag{4.11}$$

The $M(RT)^2$ algorithm is a biased random walk in configuration space; as usually carried out, each particle is moved one after another to a new position uniformly distributed inside a cube of side s. That move is either accepted or rejected depending on the magnitude of the trial function at the new position compared with the old position. Suppose $\underline{R}$ is the old position and $\underline{R}'$ the new. Then if $|\psi_T(\underline{R}')|^2 \geq |\psi_T(\underline{R})|^2$ the new point $\underline{R}'$ is accepted. Otherwise the new point is accepted with probability q where

$$q = \frac{|\psi_T(\underline{R}')|^2}{|\psi_T(\underline{R})|^2} \quad . \tag{4.12}$$

It has been shown elsewhere in this book (cf. Sect.1.2) that under certain very general conditions, the points of the random walk have $|\psi_T(\underline{R})|^2$ as their density, asymptotically as the number of steps increases.

In general the algorithm is very simple to program and test, and follows very closely a Monte Carlo simulation of a classical system. However, there are a number of things specific to quantum systems which we wish to draw to the attention of the reader who is interested in doing such a calculation.

a) Finite System Size

Usually one wishes to calculate the properties of an infinite homogeneous system but practical simulations are limited to about several thousand particles with current computers. Periodic boundary conditions are used to eliminate surface effects. Quantum systems, in general, have smaller size dependence than classical systems (see below, Sect.4.2.2). The two-particle correlation function, g(r), for liquid helium looks very much like that of a classical gas near its critical point

in that the correlations are of fairly short range. The energy per particle of 32 helium atoms (at equilibrium density) is only about 0.15 K lower than for 862 atoms out of a total potential energy of -18 K. The most serious long-range problem is that posed by the Coulomb potential, but that, as we shall see, seems to be satisfactorily solved by the use of the Ewald image potential, at least for single component systems. There, also 32 particles give reasonably good estimates for bulk properties and a few calculations with much larger systems, say 256 particles, give a good idea of the size dependence.

b) The Random Walk

For quantum systems, there seems to be no problem with the random walk converging to the desired probability distribution. The initial step of the random walk can be taken with particles on lattice sites, or uniformly distributed throughout the simulation box, or the last step of another random walk. Then typically 50 to 500 moves per particle are sufficient to ensure that the random walk converges to the distribution p(R). The step size of the random walk s is adjusted so that the acceptance ratio for moves is between 0.1 and 0.7. The smaller acceptance ratios are probably more desirable to insure rapid convergence and also save some computer time for Fermi trial functions. After the system has "equilibrated", the random walk continues, with various averages being kept, until either computer time is exhausted or the statistics are judged acceptable, preferably the latter.

c) Computation of the Pseudopotential

At each step of the random walk the relative change in the trial function must be computed to determine q in (4.12). If particle i is being moved and $\underline{r}_i'$ is its new trial position, then for the boson liquid trial function, (4.2), this is simply

$$q_B = \exp\left\{ \sum_j \left[u(\underline{r}_i - \underline{r}_j) - u(\underline{r}_i' - \underline{r}_j) \right] \right\} , \quad j \neq i \quad . \tag{4.13}$$

Then to move one particle takes computer time proportional to the number of particles. If u(r) is a short-ranged function, enumeration of nearest neighbors of each particle can be used to reduce this time to a constant, for large enough systems [4.14].

Care must be taken to avoid the use of pseudopotentials which are discontinuous, since the variational principle requires continuity of trial function and its derivative. A simple way of truncating the pseudopotential at the edge of the box is as follows. Suppose L is the length of the smallest side of the simulation cube. Then a continuous truncated potential is

$$u_T(r) = \begin{cases} u(r) - u(r_T) & , \quad r < r_T \\ 0 & , \quad r \geq r_T \end{cases} \tag{4.14}$$

where r_T is less than or equal to L/2. This potential will have a discontinuous derivative at r_T which gives rise to an easily calculated 'tail' correction to the kinetic energy. The same remarks apply to the single particle localization function $\phi(r)$ in the solid trial function [see (4.4)]. It is important to keep $\phi(r)$ smooth if the particles are only weakly localized about their lattice sites and the system is small.

On the other hand for charged systems it is often necessary to have a long-ranged 'plasmon' trial function (4.7) and truncation is not desirable. In this case one can use the Ewald image potential where the sum in (4.13) is over all of the other particles and all of their images in the periodically extended space. (See the review by VALLEAU and WHITTINGTON [4.15] for a discussion of the theory, implementation, and difficulties of Ewald sum techniques).

d) Fermion Trial Function

The presence of the Slater determinant in the Fermion trial function (4.3) complicates the random walk somewhat since one must compute the ratio of two determinants, in addition to the pseudopotential, at each step of the random walk. The additional computation can be done in the following way. At the beginning of the random walk the inverse matrices to the Slater matrices are found (one for each spin degree of freedom). That is let

$$D_{ik} = \exp(i\underline{k}\cdot\underline{r}_i) \tag{4.15}$$

be the Slater matrix and the inverse matrix $\bar{D}$ is such that

$$\sum_{k=1}^{N} D_{ik}\bar{D}_{jk} = \delta_{ij} \quad . \tag{4.16}$$

The crucial observation is that when only one particle is moved, just one row of the Slater matrix changes, the matrix of cofactors for that row is unchanged, and one can compute the ratio of determinants by a simple scalar product. That is,

$$q = q_B \times \left| \sum_{k=1}^{N} \exp(i\underline{k}\cdot\underline{r}_i')\bar{D}_{ik} \right|^2 \quad , \tag{4.17}$$

where q_B is still given by (4.13). If the move is accepted, the inverse matrix needs to be updated and this takes roughly N^2 operations on the computer [4.16]. Because of the necessity of storing and updating the inverse matrices, it is more difficult to do a large fermion system than a large bose system. A random walk with 250 particles is a substantial calculation, but such a system is sufficiently large for particles interacting with a short-range potential [4.16]. That is, the dependence of the energy on the size of the system for 250 particles is usually comparable to the statistical error and much smaller than error of using the trial function (4.3). The electron gas in the range of metallic densities has important size dependence, even after using the Ewald image potential. But most of this error can be eliminated [4.17].

e) Computing the Trial Energy

The most important average to be done with Monte Carlo is the trial energy since it must be minimized with respect to u(r). Green's theorem can be used to cast the energy into several different forms and to check on the convergence of the random walk.

The following relation holds for continuous trial functions with periodic boundary conditions

$$- \int d\underline{R}\ \psi_T^* \nabla^2 \psi_T = \int d\underline{R} |\psi_T|^2 \quad |\nabla \ln \psi_T|^2 \quad . \tag{4.18}$$

Then for the boson liquid trial function the variational energy can be rewritten as

$$E_B = \frac{\int d\underline{R} |\psi_T(\underline{R})|^2 \sum_{i<j} \left[v(r_{ij}) + \frac{\hbar^2}{4m} \nabla^2 u(r_{ij}) \right]}{\int d\underline{R} |\psi_T(\underline{R})|^2} \tag{4.19}$$

and the trial energy can be calculated once the radial distribution function, g(r), is known. For an N body system in volume V,

$$g(\underline{r}) = \frac{V(1 - 1/N) \int |\psi_T(\underline{R})|^2 \delta(\underline{r}_i - \underline{r}_j - \underline{r}) d\underline{R}}{\int |\psi_T(\underline{R})|^2 d\underline{R}} \quad . \tag{4.20}$$

For fermions, different distribution functions can be defined for particles of the same or opposite spins.

It does not seem to be generally realized that this transformed estimator for the energy has a serious drawback. The original form for the energy, (4.1), has a zero variance in the limit as ψ_T approaches a solution of the Schrödinger equation. That is, for any point $\underline{R}_i$, $\psi_T^{-1}(\underline{R}_i)\, H\psi_T(\underline{R}_i)$ will always have the same value and there is no sampling error. In practice, we have found that the standard error obtained using form (4.1) of the energy is at least four times smaller than that from the transformed form in (4.19) for liquid helium and the electron gas.

The second relationship, due to FEYNMAN [4.10], is applicable whenever the trial function can be split into two parts. Suppose

$$\psi_T(\underline{R}) = A(\underline{R})B(\underline{R}) \tag{4.21}$$

then

$$-2 \int d\underline{R}\; AB\underline{\nabla}A\cdot\underline{\nabla}B = \int d\underline{R}(|\underline{\nabla}A|^2 + A\nabla^2 A)B^2 \tag{4.22}$$

$$= \int d\underline{R}(|\underline{\nabla}B|^2 + B\nabla^2 B)A^2$$

Together with (4.18) we can transform the kinetic energy of the fermion trial function into many different forms but again we will in general raise the variance of the trial energy as compared to the use of (4.1). Expressions (4.18,22) are useful, however, as a check of the convergence of the random walk.

Finally we should mention that scaling can be used to relate the value of the energy at one density to its value at another density. Let 'a' stand for the set of all parameters in the trial function having units of length. Then clearly the two-particle correlation function scales in the following way

$$g(r/\ell,\rho',a/\ell) = g(r,\rho,a) \quad \text{where } \ell = (\rho'/\rho)^{1/3} \quad . \tag{4.23}$$

Now (4.19) shows that the energy for bosons can be written as an integral over g(r). Of course, the optimum trial parameters at one density will not usually scale into optimum trial parameters at another density but the scaling helps locate the minimum energy.

f) The Pressure

For any equilibrium system the virial theorem gives the pressure once the kinetic energy T and the radial distribution function are known.

$$P = -\frac{1}{N}\frac{\partial E}{\partial \rho} = \frac{\rho}{3}\left[2T - (\rho/2)\int d^3r\; g(r)\; r\,\frac{dv}{dr}\right] \quad . \tag{4.24}$$

This relation has occasionally been used to check the accuracy of variational calculations. But a proof based on a scaling argument quoted by COCHRAN [4.18] shows that the virial theorem also holds for variational energies. More precisely, the two pressures in (4.24) will be equal if all lengths in the trial wave function are considered as parameters and $E(\rho)$, $T(\rho)$ and $g(r,\rho)$ are evaluated at the variational minimum of these parameters.

g) The Single Particle Density Matrix

The single-particle density matrix $n(r)$ and its Fourier transform, the momentum density $n(k)$, can be easily computed from the product trial function as sampled by the random walk. The function $n(r)$ is defined as

$$n(r) = \frac{\int d\underline{R}\ \psi_T^*(\underline{r}_1 + \underline{r}, \underline{r}_2, \ldots, \underline{r}_N)\psi_T(\underline{r}_1, \underline{r}_2, \ldots, \underline{r}_N)}{\int d\underline{R} |\psi_T|^2} \quad . \tag{4.25}$$

For large r in a Bose liquid, $n(r)$ will go asymptotically to the condensate fraction [4.19], the fraction of particles in the zero momentum state. Furthermore, the probability density for finding a particle with a wave vector k is simply

$$n(k) = \rho \int d^3r\ e^{i\underline{k}\cdot\underline{r}} n(r) \quad . \tag{4.26}$$

An ingenious and very efficient way of carrying out the averages in (4.25,26) is due to McMILLAN [4.1]. A point $\underline{r}'$ is selected uniformly inside the simulation box where the random walk is taking place. That point is successively considered to be each of the particles in turn, displaced an amount $\underline{r}' - \underline{r}_i$. Then

$$n(|\underline{r}' - \underline{r}_i|) = \left\langle \frac{\psi_T(\underline{r}_1, \ldots, \underline{r}', \ldots, \underline{r}_N)}{\psi_T(\underline{r}_1, \ldots, \underline{r}_i, \ldots, \underline{r}_N)} \right\rangle \quad . \tag{4.27}$$

If the calculation is correctly arranged, only one distance and exponential need be computed for each value contributing to the average of $n(r)$.

h) Reweighting Configurations

If one has available configurations generated from one trial function it is relatively simple to calculate properties, such as the energy, of a slightly different trial function. Suppose $\{\underline{R}_i\}$ is a set of configurations drawn from the probability

distribution $|\psi_T(\underline{R},\underline{a})|^2$. Then clearly one can calculate averages from a different trial function $\psi_T(\underline{R},\underline{a}')$ as follows

$$\langle A(\underline{a}')\rangle = \frac{\int \psi_T^*(\underline{R},\underline{a}')A\,\psi_T(\underline{R},\underline{a}')d\underline{R}}{\int |\psi_T(\underline{R},\underline{a}')|^2 d\underline{R}}$$

$$= \frac{\lim_{M\to\infty}\left\{\sum_{i=1}^{M} W_i \psi_T^{-1}(\underline{R}_i,\underline{a}')A\psi_T(\underline{R}_i,\underline{a}')\right\}}{\sum_{i=1}^{M} W_i} \qquad (4.28)$$

where the weights W_i are

$$W_i = \frac{|\psi_T(\underline{R}_i,\underline{a}')|^2}{\psi_T(\underline{R}_i,\underline{a})|^2} \quad . \qquad (4.29)$$

For this procedure to be reliable it is important that I) there be a large number of configurations, at least several hundred to eliminate bias in the estimates, and II) that all the weights be of the same order of magnitude, i.e., the largest weight be no more than that roughly 5 times larger than the mean weight. If the second condition is not satisfied it means that there is probably not enough overlap between the trial functions for the procedure to be successful. We have found this procedure allows one to compute the changes in energy due to a change in trial function parameters much more accurately and quickly than doing two separate random walks and subtracting the energies, since in the former case the estimates are positively correlated and in the latter they are not.

4.2.2 Application to Systems of Helium

The first reported use of the Metropolis random walk for a quantum system was by McMILLAN [4.1] for the ground state of liquid helium four. Independent and almost identical calculations were done at about the same time by LEVESQUE et al. [4.20]. Since that time simulations have been done for many simple quantum many-body systems. We will review most of these papers, and indicate some of what has been learned from the studies. The review is organized into three sections: hard-core boson systems, soft-core (including Coulomb) boson systems, and fermion systems.

a) Hard-Core Boson Systems

For our purposes, a hard-core system is one for which the radial distribution function is essentially zero for small r. It is generally believed that all substances in nature do not really have a hard core, but at normal densities atomic systems behave as if they did.

The physical difference between hard-core potentials and soft-core potentials is the behavior at increasing density. The energy and pressure of hard-core systems will increase very rapidly as soon as the cores begin to overlap and as a consequence they will solidify. But the potential energy of a soft-core system only increases with some power (less than one) of the density, the kinetic energy becomes dominant, and as a consequence it will melt at high density. Among atomic substances, only the lightest show significant macroscopic quantum effects at low temperatures. They are shown in Table 4.1 (from STWALLEY and NOSANOW [4.21]). The three isotopes of hydrogen, H↑, D↑ and T↑ are assumed 'spin-aligned'; a very strong magnetic field ($\sim 10^5$ G) forces all of the electrons to have the same spin, thus preventing molecules from forming. The interatomic potentials have all been fit by a Lennard-Jones 6-12 potential,

$$v(r) = 4\underline{\varepsilon}[(\underline{\sigma}/r)^{12} - (\underline{\sigma}/r)^{6}] \tag{4.30}$$

using virial data (ε and σ are shown in Table 4.1). The measure η was introduced by DE BOER [4.22] in his quantum theory of corresponding states and is given by

$$\eta = \hbar^2/m\varepsilon\sigma^2 \quad . \tag{4.31}$$

Essentially η will be the ratio of the zero-point kinetic energy and the classical potential energy and thus determines the importance of quantum effects at zero temperature. It is obvious that the thermodynamic properties for any Lennard-Jones system are only determined by η, the reduced density $\rho\sigma^3$, and the reduced temperature kT/ε.

The ground-state energies of all of the atomic systems in Table 4.1 have been calculated using Monte Carlo techniques. ^{4}He is the most popular and we will discuss it first.

b) Liquid ^{4}He

McMILLAN [4.1] did the original simulation of liquid ^{4}He and many others have extended and reproduced his results.

Table 4.1 The atomic substances which show sizable quantum effects at zero temperature. The hydrogen isotopes are spin aligned, placed in a magnetic field strong enough so that all electrons are in one spin state. ε and σ are the parameters of an effective Lennard-Jones 6-12 potential, η is de Boer's quantumness parameter

Substance	Mass	ε	σ	$\eta=\hbar^2/m\varepsilon\sigma^2$	Ground state
H↑	1	6.46	3.69	0.55	Bose gas
D↑	2	6.46	3.69	0.27	Fermi gas or liquid?
T↑	3	6.46	3.69	0.18	Bose liquid
^{3}He	3	10.22	2.556	0.2409	Fermi liquid
^{4}He	4	10.22	2.556	0.1815	Bose liquid
^{6}He	6	10.22	2.556	0.1207	Crystal
H_2	2	37.00	2.92	0.0763	Crystal
D_2	4	37.00	2.92	0.0382	Crystal
Ne	20	36.2	2.744	0.0085	Crystal

I) *Direct Application of Monte Carlo.* McMILLAN used the form

$$u(r) = (b\sigma/r)^m \quad . \tag{4.32}$$

Notice that if m = 5, u(r) will satisfy, to leading order, (4.5) for the small r behavior with $b = (16/25)^{1/10} = 1.134$ (independent of density). Also note that unless m = 2 this wave function cannot give the correct long-range behavior and S(k) will not be linear at small k. The pseudopotential admits a very simple form of scaling; only the moments $\Phi_n(b) = \langle(\sigma/r_{ij})^n\rangle$ need be obtained (n = m + 2,6,12) in order to scale to any density, while for a general pseudopotential the full g (r) is needed. McMILLAN found that m = 5 gives the lowest energy, with the value of $b = 1.17$. This was confirmed by SCHIFF and VERLET [4.23], and by MURPHY and WATTS [4.24] in more accurate calculations.

McMILLAN found the zero pressure density to be 0.89 ± 0.01 of the experimental value and the energy at that density was (-5.9 ± 0.1) K. The experimental value is -7.14 K. The fraction of particles in the zero momentum state (n_0) was found to be 0.11 ± 0.01.

The size dependence in these numbers was found to be very small. McMILLAN could find no difference between a 32 and a 108 particle system. SCHIFF and VERLET with a much larger system (864 particles) again found the same energy within statistical errors. Combining these results we believe the size effects in the energy are probably less than 0.15 K for a 32 body system.

There are several ways these calculations have been enlarged upon: by looking at approximate integral equations, looking for better pseudopotentials and trying to invert the potential.

II) *Integral Equations*. The first comparison with Monte Carlo was done by LEVESQUE et al. [4.20]. Their results showed that the Percus-Yevick equation gives energies -2 K below the Monte Carlo and has the wrong density dependence (gets worse at higher densities). The PY2 equation gives an error of about -1 K. The hypernetted chain integral equation has energies about 1.0 K too high at ρ_0 and 3.4 K too high at $\rho = 0.028$ [4.24,25]. The equilibrium density is an extremely sensitive measure of how well the equations of state are calculated. The HNC gives an equilibrium density which is only 0.8 of the value obtained from Monte Carlo. The g(r) obtained from HNC is quite reasonable but the relatively large cancellation of potential and kinetic energy means that for helium one cannot resolve energy differences of less than 1 K with integral equations. This is a serious limitation.

III) *The Optimum Pseudopotential*. It is clear from the discussion after (4.6) that the simple form used by McMILLAN for u(r) cannot be optimal. However, attempts to improve it have generally failed. It is known that for large r, u(r) is proportional to $1/r^2$ as in (4.6). SCHIFF and VERLET [4.23] tried to add a long-range term using perturbation theory, the energy was indeed lowered, but apparently the perturbation theory is not accurate enough as the energy decreases without bound. ZWANZIGER [4.26] actually added a term like

$$u(r) = \frac{mc}{\rho\pi^2\hbar} \frac{1}{r^2 + 1/k_c^2} \tag{4.33}$$

to his trial function in the Monte Carlo calculation using the Ewald image potential. The results were somewhat inconclusive due to poor statistics but roughly, the optimum value of b was unchanged from the value at $k_c = 0$, namely 1.17. c was not varied but assumed to be the experimental speed of sound. The optimum value for k_c was found to be $0.45/\text{Å}$, and the energy was lowered roughly -0.2 K. The equilibrium density and superfluid fraction remained constant within the errors. Other authors have presented other pseudopotentials with different short-range behavior. The one of de MICHELIS and REATTO [4.27] is notable in having 8 variational parameters. However, in no case is the energy lowered significantly (more than 0.2 K) [4.20,27, 28,29]. Recently CHANG and CAMPBELL [4.25] have published the best pseudopotential for the HNC equation, obtained with the use of the 'paired phonon' method. Their optimized u appears to be a short-range part as in (4.32) and the long-range part from (4.33) with the same coefficients. Here again, however, the energy in going from the simple $1/r^5$ to the most general form of u only drops by 0.14 K at ρ_0 and somewhat more at higher densities. We conclude that the 1 K difference between the Monte Carlo results and the experiment is not due to the particular form of the pseudopotential. We shall see that most of the difference can be accounted for by going beyond the product trial function to the exact ground state.

c) Solid ^{4}He and ^{3}He

We include the two isotopes of helium together since, as we shall see, the exchange effects are quite small in the crystal phase so that particle statistics have very little effect on the ground-state properties.

LEVESQUE et al. [4.20] and HANSEN and LEVESQUE [4.30] have done calculations with the solid product trial function in (4.4), with a gaussian localization orbital,

$$\phi(r) = \exp[-(A/2)r^2] \tag{4.34}$$

and only the unit permutation which appears in the sum of (4.4) is allowed. This trial function is then neither symmetric nor antisymmetric. They determined that the localized trial function has lower energy than the liquid one at high density and that the transition density is in good agreement with the experimental values for ^{3}He and ^{4}He.

For solid ^{4}He, a minimum density of $0.45\sigma^{-3}$ was found, compared to an experimental value of $0.468/\sigma^3$. For ^{3}He the variational result was $0.42/\sigma^3$, close to the experimental value of $0.41/\sigma^3$. The other important findings were that the density distribution around a lattice site is closely approximated by a gaussian and the rms deviation divided by the nearest-neighbor distance, (Lindemann's ratio: γ) is about 0.27 at melting.

HANSEN [4.31] was able to find the structural transition HCP-BCC in solid ^{3}He using Monte Carlo and found $V_{HCP/BCC} \approx 21.8$ cm^3/mole. This agrees well with experiment, $V_{HCP/BCC} = 19.8$ cm^3/mole but the calculated pressure is half the experimental value. Thus the liquid and solid product trial functions have been able, at least qualitatively, to account for the phase transitions in the two isotopes of helium.

HANSEN and POLLACK [4.32] have investigated a wider class of trial functions for the solid having the form

$$\psi_T = \exp\left\{-\frac{1}{2}\sum_{i<j} u(r_{ij}) + (\underline{r}_i - \underline{s}_i)\underline{\underline{G}}_{ij}(\underline{r}_j - \underline{s}_j)\right\} \tag{4.35}$$

where $\underline{s}_i$ is the set of lattice points (BCC) and $\underline{\underline{G}}$ is a tensor acting only between nearest and next-nearest neighbors. One additional parameter was introduced. However, the additional freedom in the trial function did not lower the energy significantly. They also established that the rms deviations from the lattice states were in rough agreement with the experimental values estimated from the Debye temperature, for both isotopes of helium, the variational estimates being 5 to 20% too small. This kind of comparison which is based on a harmonic model of a solid is not conclusive.

d) Interatomic Helium Potential

The interaction between the helium atoms in all of the above was assumed to be Lennard-Jones with ε and σ given in Table 4.1. Once a variational calculation has been done it is relatively straightforward to find the equation of state for a slightly different potential and thus try to determine from the variational results at zero temperature the interatomic potential.

A potential can be accepted only if the variational energies are greater than the experimental energies at all densities. In this way the Haberlandt potential [4.33] can be rejected from the liquid helium variational calculations [4.23]. Also the energy of the Lennard-Jones 9-6 potential with the Kihara parameters lies below the experimental solid helium energies [4.34]. Another test is to require that the pressure, estimated using a given potential, agree roughly with experimental pressures throughout a large density range, particularly in the high-density solid. This assumes that the errors made in using the product trial functions are roughly independent of density. We will discuss this below. Using this test, HANSEN [4.32,34] showed that a Lennard-Jones 6-12 potential with slightly changed coefficients (ε = 10.2 K, σ = 2.62 Å), the Morse potential of BRUCH and McGEE [4.35], and the Beck potential [4.36], are significant improvements. There is a significant improvement in the structure functions with these potentials as well [4.37].

The potential energy of a group of helium atoms cannot be expected to be exactly equal to a sum of two-body potentials; three and more body interactions are known to exist. It is possible to estimate the perturbational effect of a specific form. The most videly used three-particle interaction is the long-range triple dipole or AXILROD-TELLER [4.38] interaction

$$v_3(r_1,r_2,r_3) = u_0(1 + 3\cos\theta_1\cos\theta_2\cos\theta_3)/r_{12}^3 r_{13}^3 r_{23}^3 \quad . \tag{4.36}$$

The angles θ are the internal angles of the triangle (r_1,r_2,r_3) and u_0 = 0.324 K. MURPHY and BARKER [4.39] have calculated the energy of this term in liquid ^{4}He with the McMillan pseudopotential (4.32) and found it to be $0.14(\rho/\rho_0)^3$ K (ρ_0 is the liquid equilibrium density). Their estimate for solid ^{4}He is $+0.10\ (\rho/\rho_0)^3$ K. This is a rather small energy compared with the 1 K energy difference between the various two-body potentials.

e) The Hard-Sphere Potential

The hard-sphere model has had considerable success in explaining the structure and liquid-solid transitions of classical systems. It is natural to inquire what the zero temperature properties of a system of hard spheres are. A variational calculation has been done by HANSEN et al. [4.40] using the correlation function

$$\exp\left[-\frac{1}{2}u(r)\right] = \tanh\{[(r/a)^m - 1)]/b^m\} \tag{4.37}$$

where a is the hard-core diameter. They obtained a solidification density of $0.23/a^3$ and a melting density of $0.25/a^3$. With the choice of a = 2.556 Å both the crystallization density and the structure function agree roughly with the experimental value for helium 4.

KALOS et al. [4.28] have shown that a perturbation formula from classical liquid theory [4.41] can be used to calculate the energy of a Lennard-Jones liquid from the Monte Carlo results of the hard-sphere liquid. The Lennard-Jones potential is split into an attractive part w(r) and a purely repulsive part $v_{LJ}(r) - w(r)$. Let

$$w(r) = \begin{cases} -\varepsilon & r < r_m \\ v_{LJ}(r) \quad , & r \geq r_m \end{cases} \tag{4.38}$$

where $-\varepsilon$ is the minimum value of $v_{LJ}(r)$ and r_m is the separation at which it is attained. Then they showed that the variational energy of the Lennard-Jones liquid is given by

$$E_{LJ} = E_{HS}(a_{LJ}) + (\rho/2)\int d\underline{r}\; g_{HS}(r/a_{LJ})w(r) \tag{4.39}$$

where E_{HS} and g_{HS} are the variational hard-sphere energy and correlation function and the hard-sphere radius a_{LJ} is equal to the scattering length of the repulsive part of the Lennard-Jones potential $[v_{LJ}(r) - w(r)]$, i.e., 0.8368σ.

f) Nonuniform Helium Systems

We have seen that bulk helium can be well understood by variational calculations. LIU et al. [4.42,43] have treated two nonuniform systems with the variational method. With nonuniform problems one must generalize the product wave function to include a one-body term since otherwise a purely repulsive pseudopotential will cause the particles to fill any volume.

In the "channel" problem hard walls are placed at z = 0 and z = L, with periodic boundary conditions in the x and y directions. LIU et al. [4.42] chose to model liquid helium with hard spheres, since they were primarily interested in the structure of the system. Their trial wave function was the liquid product function times a single-particle term to make the wave function vanish at the walls.

$$\psi_T(\underline{R}) = \exp\left[-\frac{1}{2}\sum_{i<j} u(r_{ij}) \prod_{i=1}^{N} h(z_i)\right] \tag{4.40}$$

where u(r) is given by (4.37) and

$$h(z) = \tanh^q[z(L - z)/Ld] \quad . \tag{4.41}$$

We now have two additional variational parameters, q and d, to be optimized. The surface energy was found to be $0.24\hbar^2/ma^4$ which is in rough agreement with experiment. The most striking features of the results are the pronounced density variations across the channel. The quantum liquid forms a layered structure much like a classical liquid would in a channel. The number of particles in the zero momentum state remains at 11%.

The second nonuniform system that LIU et al. studied [4.43] was a double-sided film of helium. Since in order for the film to be stable, the interatomic potential must be attractive, the potential was assumed to be Lennard-Jones with ε and σ given in Table 4.1. At zero temperature all of the particles are bound to the film, so the wave function must vanish if any atom leaves the film. Their trial function had the form of (4.40) but now u(r) is the McMillan pseudopotential, (4.32), and h(z) is

$$h(z) = \begin{cases} 1 & |z| < z_0 \\ 2/[1 + \exp \kappa(|z| - z_0)^2] \quad , & |z| \geq z_0 \end{cases} \tag{4.42}$$

z_0 and κ are optimized to find the lowest energy. The surface energy was found to be 0.21 $K/\text{Å}^2$, only 25% lower than the experimental value, 0.27 $K/\text{Å}^2$. The density oscillations are much smaller in the film than in the fluid but still apparent.

g) Two-Dimensional Helium

If helium atoms are tightly bound to a surface then one has essentially a two-dimensional system. The simplest assumption for the effect of the substrate is that the helium atoms are confined to a plane and the potential felt by the helium atoms due to the substrate is constant. The helium-helium interaction may be taken to be Lennard-Jones, (4.30). HYMAN [4.44] using the Monte Carlo variational technique and CAMPBELL and SCHICK [4.45] using molecular dynamics (both used the McMillan r^{-5} pseudopotential) have calculated the equation of state in the liquid phase at zero temperature of this 2-D system. The two calculations are in agreement giving an equilibrium (zero presure) density of $\rho = 0.23/\sigma^2$ with a binding energy E = 0.6 K. LIU et al. [4.46] have calculated the energy in the solid phase (by MC) and determined that the system melts at $\rho = 0.46/\sigma^2$ and freezes at $0.40/\sigma^2$ in rough agreement with experiments on thin helium films. They also found that 38% of the atoms were in the zero momentum state at the liquid equilibrium density. This

is a much higher fraction of condensate at the equivalent density than in the three-dimensional liquid.

h) Three-Body Pseudopotential

An interesting calculation was done for this two-dimensional Lennard-Jones system by WOO and COLDWELL [4.47] who included a three-body pseudopotential in the trial function. That is they calculated the variational energy of the trial function

$$\psi_T(\underline{R}) = \prod_{i<j} \exp\left[-\frac{1}{2} u(r_{ij})\right] \prod_{k<\ell<m} \exp\left[-\frac{1}{2} w(r_{k\ell}, r_{\ell m}, r_{mk})\right] \tag{4.43}$$

where u(r) is the usual McMillan pseudopotential and w has the form

$$w(r,s,r-s) = \{c/[r^2 + s^2 + (r-s)^2]\}^{n/2} \quad . \tag{4.44}$$

This trial function will favor configurations of particles forming equilateral triangles. Thus the potential energy will be lowered, since particles will be in the potential wells of their nearest neighbors. Configurations were sampled with the usual two-particle trial functions and then the change in energy was calculated for a variety of values of c by 'biased selection'. They find an energy drop of 0.12 ± 0.06 K but the statistical errors seem rather large. Since the exact ground-state energy is not known in two dimensions it is difficult to know whether the form of their trial function is significantly better than McMillan's trial function.

CHANG and CAMPBELL [4.25] using the convolution approximation for the three-body correlation function have optimized the $w(r_{12}, r_{13}, r_{23})$ for liquid helium in three dimensions. The energy drops by -0.44 K at the equilibrium density and more at higher density when this three-body trial function is included (see also [4.48]). As we shall see, the ground-state energy is roughly 0.6 K lower than this. Either the convolution approximation is inaccurate or higher terms than the three-body function are necessary to describe liquid helium accurately. However, it is clear that the energy can be significantly lowered by relaxing the two-body approximation.

4.2.3 Other Bose Systems

a) Spin-Aligned Hydrogen

The ground-state energy for spin-aligned hydrogen and tritium has been calculated by DUGAN and ETTERS [4.49] using Monte Carlo with the liquid trial function. The potential was taken to be the Morse form

$$v(r) = \varepsilon\{\exp[2c(1 - r/r_m)] - 2\exp[c(1 - r/r_m)]\} \tag{4.45}$$

with $\varepsilon = 6.19$ K, $c = 6.05$ and $r_m = 4.15$ Å.
The pseudopotential which they found to have the lowest energy has the form

$$u(r) = b_1 \exp(-b_2 r) \quad . \tag{4.46}$$

The optimal coefficients were within 10% of those which satisfy the small r condition of (4.5). DUGAN and ETTERS found that at low pressures, spin-aligned hydrogen is nearly an ideal Bose gas and tritium a liquid, most likely superfluid. DANILOWICZ et al. [4.50] have calculated the phase transition between gas and solid aligned hydrogen to be at 80 atm with a volume of 55 cm^3/mole. At present there are no experimental values.

The atomic hydrogen potential has been fit to a Lennard-Jones 6-12 potential by STWALLY and NOSANOW [4.21]; cf. [4.51]. They have extended the moment functions $\Phi_n(b)$ for McMillan's trial functions (4.32) with m = 5 and fitted them with polynomials. Then the optimum variational energy as a function of density can easily be obtained from those moment functions. They get good agreement with Dugan for spin-aligned hydrogen.

A series of papers by NOSANOW et al. [4.52] has treated an entire range of Lennard-Jones potentials (i.e., the η,ρ^* plane) by assuming the pseudopotential was always $(b/r)^5$. Points not available from SCHIFF and VERLET [4.23] were evaluated by additional Monte Carlo calculations.

They have determined that for $\eta < 0.456$, the zero pressure phase of Lennard-Jones bosons is a liquid, and for $\eta > 0.456$ it is a gas. There is no 'coexistence' region in this hypothetical phase diagram; that is, there is no Lennard-Jones potential which has as its zero pressure ground-state liquid and gas in equilibrium. For fermions they believe the equilibrium situation is possible.

Finally the two quantum crystals, molecular hydrogen and neon have been investigated by Monte Carlo. HANSEN [4.53] found that solid neon is well described by the Hartree theory and he obtained very good agreement with the experimental ground-state energy using a Lennard-Jones potential. BRUCE [4.54] also approximated the potential between two hydrogen molecules by a Lennard-Jones (with the ε and σ in Table 4.). He argues that this approximation is not too unrealistic for solid hydrogen. He finds rough agreement with the experimental equation of state and determines that the harmonic approximation is good at high densities. For a comparison of these Monte Carlo results with those of lattice dynamics see the review by KOEHLER [4.55].

b) Soft-Core Bose Systems

We now turn to Monte Carlo results on soft-core systems. By soft core we mean here that the interparticle potential goes as +1/r for small r. In contrast to hard-core systems, the liquid or gas phase is favored at high density. There are three important systems that have been studied: the Bose one-component plasma, boson neutron matter, and the related Yukawa potential.

c) Bose Neutron Matter Calculations

Since the late 1960s it has been speculated that the interior of neutron stars and in particular pulsars is composed of neutron matter which has crystallized. See the review of BAYM and PETHICK [4.56] for background on this problem. However, different methods gave widely varying answers for the equation of state and transition density and it was proposed that a common simplified potential be chosen so that the various many-body methods could be compared. Thus the 'homework' problem was to produce the equation of state and transition density of bosons interacting with the Yukawa potential.

$$v(r) = \varepsilon \exp(-r/\sigma)/(r/\sigma) \qquad (4.47)$$

with ε = 45389 MeV and σ = 0.204 fm .

COCHRAN and CHESTER [4.18,57] assumed the pseudopotential had the form of a Yukawa function

$$u(r) = A \exp(-Br)/r \quad . \qquad (4.48)$$

Using the potential parameters ε = 23472 MeV and σ = 0.244 fm, they calculated with Monte Carlo the liquid equation of state. Their solid trial function was the usual gaussian times product function (4.4,34) but they found solid energies always above the liquid. They also considered the effect of an attractive tail to the interneutron potential but again the liquid was the favored phase. PANDHARIPANDE [4.58] showed that the HNC equation reproduced the Monte Carlo energies for the homework Yukawa potential within 5%.

The Monte Carlo results were extended to the full (η,ρ^*) plane of the Yukawa potential by CEPERLEY et al. [4.59] where η is given by (4.31) and $\rho^* = \rho\sigma^3$ is the reduced density but ε and σ are now parameters of the Yukawa potential in (4.47). They found that for $\eta \geq 0.009$, no solid will form at any density. For $\eta \leq 0.009$ the solid is the preferred phase for intermediate densities ($\rho^* \approx 0.07$), and gas the preferred phase at high and low densities. But the 'homework' potential has η = 0.022 so that a solid will never be the preferred phase.

These authors also investigated the Yukawa solid in some detail. Two different types of trial functions were used in addition to the standard gaussian form. The first was the periodic solid trial function

$$\psi_T(\underline{R}) = \exp\left[-\frac{1}{2}\sum_{i<j} u(r_{ij}) - \frac{1}{2}\sum_i \phi(\underline{r}_i)\right] \tag{4.49}$$

where $\phi(\underline{r})$ is a function with the periodicity of the lattice. The minimum variational energy for the periodic trial functions are higher than those of the gaussian, apparently because the periodic function allows a much greater chance of double occupancy of the lattice site.

To get a feeling for the effect of exchange in the Yukawa crystal a Monte Carlo simulation of the symmetrized gaussian trial function was carried out. That is

$$\psi_T(\underline{R}) = \exp\left[-\frac{1}{2}\sum_{i<j} u(r_{ij})\right]\sum_P \exp\left[-\frac{A}{2}(\underline{r}_i - \underline{s}_{p_i})^2\right] \tag{4.50}$$

where $\underline{s}_{p_i}$ are the lattice sites with a permutation P in the pairing of particles to lattice sites. To sample this function with Monte Carlo a Metropolis random walk was done both in coordinate and permutation space. Interested readers can find details in [4.59]. It was found that at the optimum value of A, very few permutations are allowed and the energy is unchanged from the unsymmetrized gaussian trial function. However, at small values of A the energy of the permanent function is slightly larger than that of the gaussian function and very many permutations can exist. We conclude that to calculate most properties of the Yukawa crystal it is not necessary to symmetrize the trial function.

It was also found that Lindemann's quantum melting law holds in the Yukawa crystal. This states that the solid is the ground-state as long as the rms deviation from a lattice site is less than 0.26 of the nearest neighbor distance. For classical system this ratio is about 1/7.

Finally, it was found that attempts by others [4.60,61] to model neutron matter from the hard-sphere or Lennard-Jones Monte Carlo results, as in (4.39), led to a serious overestimation of the kinetic energy and therefore the total energy of neutron matter at high densities.

d) Bose One-Component Plasma

The one-component plasma is the other important Boson soft-core system. The particles interact with a Coulomb potential and a uniform background neutralizes the total charge. This is a model for helium ions in the interior of cold stars. The ground-state properties depend only on one parameter r_s

$$r_s = (3/4\pi\rho)^{1/3} m(Ze)^2/\hbar^2 \quad . \tag{4.51}$$

In order to screen out the effects of the long-range potential, the pseudopotential must have long range. Consideration of the plasmon modes [4.12] show that it must go asymptotically to the form in (4.7). This makes the Monte Carlo calculation somewhat more difficult since the Ewald image potential must be used to calculate both the real potential and the pseudopotential.

HANSEN et al. [4.62] made the assumption that the pseudopotential was purely coulombic, viz.,

$$u(r) = a/r \quad . \tag{4.52}$$

Then the variational energy can be computed from the classical one-component plasma energies. The solid trial function was purely harmonic – the Einstein model – and using these energies they estimated the Wigner gas-solid transition as $r_s \approx 390$.

MONNIER [4.63] used a two-parameter pseudopotential,

$$u(r) = a(1 - e^{-br})/r \tag{4.53}$$

to obtain variational energies for smaller values of r_s. However, more recent work has not reproduced his results; his method of accounting for the finite size of the system is likely in error by roughly 10%.

Recently GLYDE et al. [4.64] and HANSEN and MAZIGHI [4.65] calculated the energies with Monnier's pseudopotential (4.53), using the HNC equation to obtain the g(r). The HNC equation has proved quite accurate for the classical plasma and might be expected to be so here since the assumed pseudopotential also has a soft core. In fact this is true. Monte Carlo simulations [4.65] for the quantum one-component plasma show that the HNC energies are accurate to about 1% of the total energy. Using solid energies from the self-consistent phonon theory and liquid energies from HNC, GLYDE et al. [4.64] found the Wigner transition to be at $r_s = 135$.

The condensate fraction as computed with Monte Carlo by HANSEN [4.65] is in qualitative agreement with the prediction of the Bogoliubov theory [4.66]. The condensate fraction is rather large even in the strong coupling region, 26% at $r_s = 26$ and 1% at $r_s = 130$.

Recent Monte Carlo calculations by one of us [4.17] imply that a more accurate value of the Wigner transition is $r_s = 100$. The pseudopotential used in these calculations is interesting since there are no variational parameters at all in the liquid phase and only one in the solid. If one uses the random phase approximation and demands that the energy of the liquid or solid plasma be constant irrespective

of the phonons present, one can show [4.17] that the optimal pseudopotentials has the following form

$$u(r) = 1/(2\pi)^3\rho \int d^3k\left[-1 - 2A/k^2 + \sqrt{1 + 4A/k^2 + 4mv(k)/\hbar^2k^2}\right] \exp(ik\cdot r) \quad (4.54)$$

where v(k) is the Fourier transform of the interparticle potential. A is the localization of the gaussians in (4.34) (zero for the liquid). The variational energies with this trial function are as low as those from Monnier's pseudopotential (4.53) in the liquid and significantly lower than the self-consistent phonon theory in the solid. They agree well, however, with the anharmonic crystal calculation [4.67].

4.2.4 Fermi Liquids

We have avoided discussing Fermi liquids up to this point because the Monte Carlo simulation of fermion systems has lagged substantially behind that of boson systems. The important Fermi liquids, the electron gas, ^{3}He, and neutron and nuclear matter, are somewhat similar to, and perhaps more interesting, than their Bose counterparts. The reluctance to do Monte Carlo simulation with the fully antisymmetric trial function in (4.3) may be a consequence of the fact that there is no direct correspondence between the trial function and a classical Boltzmann distribution and also because of the feeling that computing the determinants in the trial function would be slow.

It has recently been shown [4.16] that carrying out Monte Carlo variational calculations is not substantially more difficult for the fermion trial function than for the Base case. Furthermore as we shall see it is simpler, more elegant, and above all, more reliable than the perturbative approximations made hitherto in treating Fermi liquids.

A large number of calculations have treated Fermi liquids by applying a permutation expansion due to WU and FEENBERG [4.68] to the results of a boson calculation. For this expansion, one assumes that the ground-state Fermi wave function is given by

$$\psi_F = \psi_B \cdot D \quad (4.55)$$

where ψ_B is a symmetric wave function and D is the ideal gas Slater determinant appropriate to the problem. As originally proposed by WU and FEENBERG, ψ_B was the exact boson wave function; in that case the energy for the product assumes a particularly simple form, namely

$$E_F = \frac{\int d\underline{R}\ \psi_F^* H \psi_F}{\int dR |\psi_F|^2} = E_B + \frac{\hbar^2}{2m} \frac{\int d\underline{R}\ \psi_B^2 |\nabla D|^2}{\int d\underline{R} |\psi_F|^2} \quad . \tag{4.56}$$

E_B is the exact boson ground-state energy. The second term can be expanded using methods from classical cluster series. The first term of the expansion is simply the energy of an ideal Fermi gas, $3\hbar^2 k_F^2/10m$. The second term is an integral over the exact Bose structure function, the third term an integral over the exact Bose three-particle correlation function and so on.

If E_B is replaced by the minimum Bose variational energy and the exact correlation functions are replaced in the expansion by the corresponding variational ones, then one can evaluate the first three terms of the cluster expansion with the Bose Monte Carlo method. The resulting energy will most likely be an upper bound to the ground-state energy since the replacement of the exact Bose energy by the variational is the major error for a strongly coupled Fermi liquid. This approach has been followed by NOSANOW and PARISH [4.69] for spin-aligned deuterium; and by MILLER et al. [4.52] for the full range of Fermi liquids interacting with Lennard-Jones potentials.

However, this way of treating Fermi liquids is not really variational since ψ_B is fixed to be the wave function of the Bose liquid and in general one might expect to lower the energy by allowing ψ_B to be a different trial function. If one follows this approach, as suggested by SCHIFF and VERLET [4.23], then (4.56) no longer holds and one must add more terms to the cluster expansion. SCHIFF and VERLET used this new cluster expansion for helium three [4.23] obtaining apparently good convergence. HANSEN and SCHIFF [4.70] extended these results to mixtures of helium three and helium four. MONNIER [4.63] applied the same expansion to the electron gas, and HANSEN and MAZIGHI [4.65] have recently redone his calculations.

We have mentioned only those papers using the Wu-Feenberg expansions with Monte Carlo Bose energies and correlation functions. There has been a great number of others which used integral equations to find these quantities [4.71]. Within the Wu-Feenberg theory it is impossible to judge the errors resulting from the approximations to the correlation functions and from the truncation of the perturbation expansion.

Recently we have carried out the Metropolis random walk described above for the fully antisymmetric trial function [4.16]. The liquids studied to date are ^{3}He, neutron matter, Yukawa fermions and the electron gas in two and three dimensions [4.17]. The pseudopotentials used in the trial function were identical in form to those used in the corresponding boson liquid, that is $(b/r)^5$ for helium three, the Yukawa function (4.48) for neutron matter and the Gaskell [4.72] pseudopotential for the electron gas [which is closely related to the form in (4.54)]. The

variation of the energy per particle with the size of the system is small for these liquids. The largest system simulated to date contained 162 particles, but that should not be regarded as a limit for the method.

a) Helium Three

Our simulation of liquid ^{3}He gives fair agreement with experiment (-1.3 K/particle as opposed to the experimental -2.5 K) and good agreement with the SCHIFF and VERLET permutation expansion [4.23] energies at the equilibrium density. The convergence of the expansion for the potential energy and kinetic energy separately is not nearly as good (a first-order error of 0.7 K). Also at a higher density, the Wu-Feenberg expansion underestimates the variational energy by 1.1 K. Shown in Fig. 4.1 are the spin dependent structure functions for liquid helium three at equilibrium density.

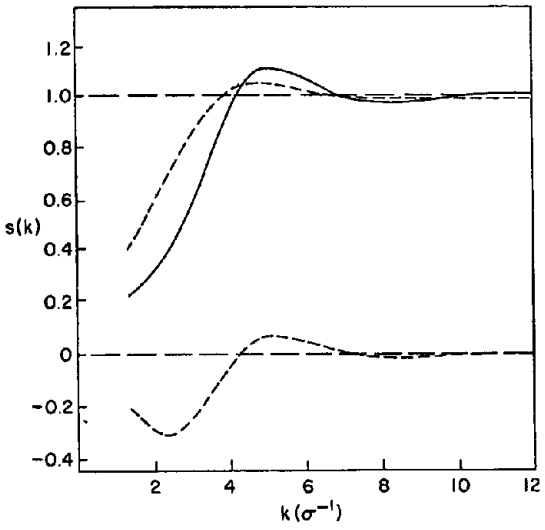

Fig.4.1 Structure functions S(k) (solid line), $S_L(k)$ (like spins upper dashed line), and S(k)-S_L(k), (lower dashed line) for liquid He-3 at a density of $0.237/\sigma^3$

b) Neutron Matter

Simulations on neutron matter show that the Wu-Feenberg expansion underestimates the variational energy at all densities. Variational calculations have been carried out with the homework potential and two different Reid potentials. The fermion 'homework' system does not crystallize at any density. A recently developed integral equation called the Fermi HNC gives good agreement with these Monte Carlo results [4.73,74] at low density ($< 0.3/fm^3$). At higher density the three different forms for the kinetic energy give widely different results indicating that the approximation has broken down. Monte Carlo calculations have provided a crucial test of these approximations [4.74].

Figure 4.2 gives the momentum distribution. One can see the residual effect of the discontinuity at the Fermi surface caused by the determinant of the trial function. The interaction excites about 23% of the particles above the Fermi surface.

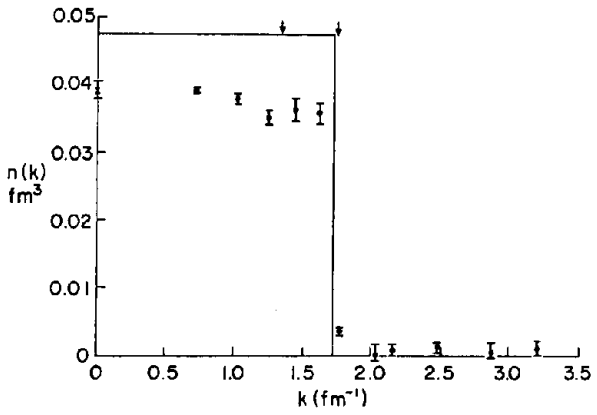

Fig.4.2 Momentum distribution, n(k) for neutron matter at a density of 0.17/fm^3. The rectangle is the ideal Fermi gas distribution. The two arrows represent the rms values of k for the ideal gas and for this model of neutron matter

c) Yukawa Fermions

We have very roughly located the gas-solid phase boundary for a system of particles interacting with the Yukawa potential (4.47) and determined that if $\eta > 0.014$ the system is always in the gas phase. This critical value of η is very near that of the homework potential ($\eta_{HW} = 0.022$); hence it is not hard to see why other, more approximate methods, might predict that the homework system solidifies.

d) The Electron Gas

The electron gas is perhaps the most studied many-body problem. Many years ago WIGNER [4.75] predicted that the system would crystallize at low density, but a consensus of opinion on the transition density has not yet been reached [4.76]. The two-dimensional electron gas is also interesting since it appears that electrons on the surface of liquid helium are nearly a perfect realization of this system [4.77] and the Wigner transition may experimentally be seen there.

A series of Monte Carlo variational calculations for this system in two and three dimensions has been carried out [4.17].

The pseudopotentials used were of two types: Monnier's form (4.55) and GASKELL's random phase' pseudopotential [4.72]

$$u(r) = \frac{1}{\rho(2\pi)^d} \int d^d k \left[-1/S_0(k) + \sqrt{1/S_0(k)^2 + 4mv(k)/\hbar^2 k^2} \right] \exp(i\underline{k}\cdot\underline{r}) \qquad (4.57)$$

where $S_0(k)$ is the ideal Fermi gas structure function and $v(k)$ is the Fourier transform of the interparticle potential. Gaskell's pseudopotential has energies as low as those using (4.53) but with the added advantage that there are no variational parameters and hence less computation. The best pseudopotential for the crystal had the form of (4.54).

Among the results for the electron gas [4.17] are the following:

I) The dependence of the energy on the size of the system is more important for the electron plasma since very small differences in energy are important. It was found [4.17] that this size dependence could be removed by interpolating between exact size dependence in the high and low density limits.

II) After the size dependence was corrected, the Monte Carlo correlation energies agree quite well with other calculations [4.78] in the metallic density range, $2 \leq r_s \leq 7$.

III) As BLOCH [4.79] predicted many years ago, using the Hartree Fock energies, the totally polarized liquid (all spins aligned) is the preferred phase at intermediate densities. In 3 dimensions the polarized-unpolarized transition should occur at $r_s = 26 \pm 5$ and in 2D at $r_s = 13 \pm 2$. This is at a substantially lower density than that predicted by other theories [4.80,81].

IV) The crystal energies are in good agreement with those calculated with the anharmonic crystal method [4.57] but substantially lower than those from the self-consistent phonon method [4.64].

V) The polarized liquid-crystal transition occurs at about $r_s = 67 \pm 5$ in three dimensions and about $r_s = 33 \pm 2$ in 2D. If the electrons are constrained to be unpolarized then the liquid-solid transition would occur at $r_s = 47 \pm 5$ in 3D and $r_s = 18 \pm 2$ in 2D. These variational estimates probably represent lower bounds to the true transition density since it is likely that the solid trial function is better than the liquid. For example, the 'exact' Bose Monte Carlo results for the Yukawa system [4.59] show the excess energy (above the perfect crystal energy) is overestimated 2% more in the liquid phase than in the crystal phase. If we shift the excess energy in the 3D electron plasma by the same percentage the polarized liquid-crystal transition goes from $r_s = 67$ to $r_s = 90$.

4.2.5 Monte Carlo Techniques for Low Temperature Excitations

Monte Carlo can be fruitfully used to calculate properties of systems which are close to the ground-state although this subject is largely unexplored.

As an example PADMORE and CHESTER [4.82] have calculated the energy of an excitation of a phonon or roton of wave vector $\underline{K}$ assuming the excited state wave function had the Feynman-Cohen form [4.83]

$$\psi_{\underline{K}}(\underline{R}) = \psi_0(\underline{R}) \sum_i \exp\left[i\underline{K}\cdot\left(\underline{r}_i + A \sum_j \underline{r}_{ij}/r_{ij}^3\right)\right] \quad .$$

Here $\psi_0(\underline{R})$ is the ground state wave function and $A(\underline{K})$ is a variational parameter. The energy of this trial function can be found from (4.56). PADMORE and CHESTER assumed $\psi_0(\underline{R})$ is approximated by the McMillan trial function and evaluated the integrals for the calculation of the energy by Monte Carlo. They were able to find the roton gap accurately in both 2 and 3 dimensions at several densities and reproduced within 20% the experimental excitation spectrum.

Two other examples of this sort of calculation can be cited. Recently SASLOW [4.84] computed an upper bound to the superfluid fraction in solid helium by a variational method suggested by LEGGETT [4.85]. The superfluid fraction in solid Yukawa bosons has been calculated in the same way, but using Monte Carlo results [4.59]. Unfortunately the bound computed this way is rather large ($\sim$ 15%) as compared with the experimental upper bounds (10^{-4}). Finally MEISSNER and HANSEN [4.86] have computed the sound velocity in solid neon, as a function of direction and density by using Monte Carlo.

4.3 Nearly Classical Systems

For systems which are almost classical, the WIGNER [4.87] $\hbar$ expansion can be used to correct classical results for quantum effects. For example, if A^c and $g^c(r)$ are the classical free energy and radial distribution function computed from Monte Carlo or molecular dynamics then the quantum free energy is

$$A/N = A^c/N + \rho\beta\hbar^2/24\, m \int d^3r\, g^c(r)\nabla^2 v(r) + O(\hbar^4) \quad . \tag{4.58}$$

The term in $\hbar^4$ involves averages over the 3 and 4 body classical distribution functions and can be evaluated with Monte Carlo [4.88]. This series seems to be quickly convergent for most fluids near their critical points. However, for very low temperatures and below the lambda transition in liquid helium it probably breaks down completeley. It is this purely quantum situation which we have been concerned with in this chapter. For a more complete discussion of the Wigner $\hbar$ expansion see [4.89].

4.4 The Green's Function Monte Carlo Method (GFMC)

a) Schrödinger's Equation in Integral Form

Consider the Schrödinger equation for a many-body system.

$$\left[-\sum_i \frac{\hbar^2}{2m}\nabla_i^2\,\psi(\underline{r}_1,\underline{r}_2,\ldots,\underline{r}_N) + V(\underline{r}_1,\ldots,\underline{r}_N)\right]\psi(\underline{r}_1,\underline{r}_2,\ldots,\underline{r}_N)$$

$$= E\psi(\underline{r}_1,\underline{r}_2,\ldots,\underline{r}_N) \tag{4.59}$$

For convenience we set $\hbar^2/2m = 1$ and let $\underline{R}$ denote the point $(\underline{r}_1,\underline{r}_2,\ldots,\underline{r}_N)$ in 3N dimensional configuration space. Then (4.59) can be written succinctly as

$$[-\nabla^2\psi(\underline{R}) + V(\underline{R})]\psi(\underline{R}) = E\psi(\underline{R}) \quad . \tag{4.60}$$

Suppose for the moment that

$$V(R) \geq -V_0;$$

we shall note later the consequences of removing this restriction. Then

$$[-\nabla^2 + V(\underline{R}) + V_0]\psi(\underline{R}) = (E + V_0)\psi(\underline{R}) \quad . \tag{4.61}$$

We seek an integral formulation of the Schrödinger equation. Accordingly, we consider Green's function for the operator on the left side of (4.61), namely

$$[-\nabla^2 + V(\underline{R}) + V_0]G(\underline{R},\underline{R}_0) = \delta(\underline{R} - \underline{R}_0) \quad . \tag{4.62}$$

Appropriate boundary conditions for the problem must be contained in G. For the treatment of an isolated system of interacting particles, $G(\underline{R},\underline{R}_0)$ vanishes as the separation of any pair of particles $|\underline{r}_i - \underline{r}_j|$ increases without limit. On the other hand in calculations modelling a large system by the use of a finite number of particles in a box of side L, ψ and G must be multiply periodic in the sense that

$$\psi(\underline{R} + \underline{P}_j) = \psi(\underline{R})$$

$$G(\underline{R} + \underline{P}_j;\underline{R}_0) = G(\underline{R};\underline{R}_0)$$

and $\underline{P}_j$ is a vector all of whose 3N components are zero except the j^{th} which is L. Finally in treating a system with hard-sphere forces,

$$\psi(R) = 0 \quad \text{if} \quad |\underline{r}_i - \underline{r}_j| \leq a, \quad \text{for any } i \neq j;$$

a is the hard-sphere diameter. In this case we require that $G(\underline{R},\underline{R}_0)$ which also vanishes when hard spheres overlap.

Substitution of the Green's function of (4.62) in (4.61) yields an integral equation

$$\psi(\underline{R}) = (E + V_0) \int G(\underline{R},\underline{R}')\psi(\underline{R}')d\underline{R}' \quad . \tag{4.63}$$

Let a succession of functions be defined for some initial $\psi^{(0)}(\underline{R})$ by

$$\psi^{(n+1)}(\underline{R}) = (E + V_0) \int G(\underline{R},\underline{R}')\psi^{(n)}(\underline{R}')d\underline{R}' \quad . \tag{4.64}$$

When the spectrum of the hamiltonian is discrete near the ground state $\psi_0(\underline{R})$ of the Schrödinger equation (4.59), then $\psi_0(\underline{R})$ is the limiting value of $\psi^{(n)}(\underline{R})$ for large n. It is possible to devise a Monte Carlo method — in the general sense of a random sampling algorithm — which produces populations drawn in turn from the successive $\psi^{(n)}$. Suppose that a set of configurations $\{R^{(0)}\}$ is drawn at random from the given function $\psi^{(0)}(\underline{R})$. Then for each configuration $\underline{R}_k^{(0)}$, let new configurations $\underline{R}_\ell^{(1)}$ be selected at random from the density function $(E+V_0)G\left(\underline{R}_\ell^{(1)}, \underline{R}_k^{(0)}\right)$conditional on $\underline{R}_k^{(0)}$. Note that the number of configurations is not conserved. The expected number of configurations appearing in a unit neighborhood of R, averaged over all possible $\underline{R}_k^{(0)}$ is

$$(E + V_0) \int G(\underline{R},\underline{R}')\psi^{(0)}(\underline{R}')d\underline{R}' = \psi^{(1)}(\underline{R}) \quad , \tag{4.65}$$

which is identical with (4.64) for n = 1. Thus the sampling of $G\left(\underline{R}_\ell^{(1)},\underline{R}_k^{(0)}\right)$produces a population of configurations $\{\underline{R}^{(1)}\}$ drawn from $\psi^{(1)}$. Clearly, repetition leads to a population whose density is $\psi^{(2)}$ and further iteration to samples drawn from $\psi^{(n)}$ for any n. We call the population drawn from $\psi^{(n)}$ the n^{th} "generation".

Unfortunately, E_0, the exact eigenvalue of the ground state, is not known in advance. Equation (4.64) requires the correct eigenvalue to yield $\psi^{(n)}$ asymptotically constant. On the other hand it is equally clear from (4.64) that if one uses, for computational purposes, a trial eigenvalue E_t larger than E_0, the $\psi^{(n)}$ will grow in normalization reflected in a growth in the population of configurations. If E_t is too small the population declines. Thus the distribution of configurations has the correct marginal distribution and, in addition, the eigenvalue E may be estimated from the change in population size

$$E + V_0 = \frac{(E_t + V_0) \int \psi^{(n)}(\underline{R})d\underline{R}}{\int \psi^{(n+1)}(\underline{R})d\underline{R}} \quad . \tag{4.66}$$

A Monte Carlo estimator for E_0 is then $\bar{E}_1$ given by

$$\bar{E}_1 + V_0 \simeq (E_t + V_0)N_n/N_{n+1} \tag{4.67}$$

where N_n is the number of configurations in the population drawn from $\psi^{(n)}$ according to (4.64) and the symbol $\simeq$ indicates that the estimates is biased. A source of bias is a consequence of the asymptotic character of the result. Another expresses the fact that the expected value of the quotient of two integrals is not the quotient of the expected values. An estimator, $\bar{E}_2$ for which the second kind of bias is smaller is

$$(\bar{E}_2 + V_0) \simeq (E_T + V_0) \sum_{k=n_1}^{n_2} N_k \Big/ \left(\sum_{k=n_1}^{n_2} N_{k+1}\right) \quad . \tag{4.68}$$

In any case the magnitude of the bias must be evaluated or bounded in obtaining practical results. Including the size of more generations decreases the bias as a consequence of the increased statistical correlation and reduced fluctuation of numerator and denominator.

The second bias can be eliminated completely and the first frequently reduced in magnitude by the following method. Multiply (4.60) by some known $\psi_T(\underline{R})$ which satisfies the boundary conditions. It has been found effective to use a trial function which minimized the energy in a variational study of the same problem. Upon integrating over the full space of $\underline{R}$ and using the Hermiticity of the hamiltonian, one obtains

$$E = \frac{\int \psi_0(\underline{R})[-\nabla^2 + V(\underline{R})]\psi_T(\underline{R})d\underline{R}}{\int \psi_0(\underline{R})\psi_T(\underline{R})d\underline{R}} \quad . \tag{4.69}$$

If one samples a population $\underline{R}_1,\ldots,\underline{R}_N$ from the density function $\psi_0(\underline{R})\psi_T(\underline{R})$ then

$$\bar{E}_3 \simeq \frac{1}{n} \sum_{k=1}^{n} \psi_T(\underline{R}_k)^{-1}(-\nabla^2 + V)\psi_T(\underline{R}_k) \tag{4.70}$$

is an unbiased estimator of E. It has the property that as ψ_T approaches ψ_0, $\bar{E}_3$ becomes exact, independent of the values of $\underline{R}_k$. Thus one expects that for "reasonable" ψ_T, the estimator $\bar{E}_3$ will be less biased than $\bar{E}_2$ before the convergence of $\psi^{(n)}$ to $\psi^{(\infty)}$ and it may well have less variance. We will discuss practical results below. Estimator $\bar{E}_2$ is called a "growth" estimate, $\bar{E}_3$ a "variational" estimate.

The iteration process (4.64) does not converge to $\psi_T\psi_0$ but, formally at least, it is easy to change it so that it will do so. Simply multiply (4.64), through by $\psi_T(R)$ and introduce $\psi_T(\underline{R}')/\psi_T(\underline{R}')$ into the integral. The sequence

$$\psi_T(\underline{R})\psi^{(n+1)}(\underline{R}) = (E_t + V_0) \int [\psi_T(\underline{R})G(\underline{R},\underline{R}')/\psi_T(\underline{R}')] \times \psi_T(\underline{R}')\psi^{(n)}(\underline{R}')d\underline{R}' \tag{4.71}$$

can be sampled randomly as before and converges to $\psi_T\psi_0$ where ψ_0 is the lowest state not orthogonal to ψ_T. The estimator (4.68) may also be used with N_k referring to the size of the population generated with the bias ψ_T. Clearly this is a practical thing to do when the sampling is carried out according to (4.71). We shall see below that this is theoretically advantageous.

We now consider the question of treating infinite attractive potentials such as occur in a two-component plasma. Suppose one writes

$$V(\underline{R}) = V_+(\underline{R}) - V_-(\underline{R}) \tag{4.72}$$

and with V_- unbounded from above, and V_+ has lower bound $-V_0$. Then (4.61) becomes

$$[-\nabla^2 + V_+(\underline{R}) + V_0]\psi(\underline{R}) = V_-(\underline{R})\psi(\underline{R}) + (E + V_0)\psi(\underline{R}) \quad . \tag{4.73}$$

Using Green's function for the operator on the left, we have

$$\psi(\underline{R}) = \int G(\underline{R},\underline{R}')V_-(\underline{R}')\psi(\underline{R}')d\underline{R}' + (E + V_0) \int G(\underline{R},\underline{R}')\psi(\underline{R}')d\underline{R}' \tag{4.74}$$

or

$$V_-(\underline{R})\psi(\underline{R}) = \int V_-(\underline{R})G(\underline{R},\underline{R}')V_-(\underline{R}')\psi(\underline{R}')d\underline{R}' + (E + V_0) \int V_-(\underline{R})G(\underline{R},\underline{R}')V_-^{-1}(\underline{R}')V_-(\underline{R}')\psi(\underline{R}')d\underline{R}' \tag{4.75}$$

an integral equation for the new dependent variable $V_-(\underline{R})\psi(\underline{R})$ which must be integrable. In some applications it is best to arrange the decomposition so that V_0 is zero and transpose $E\psi$ to the left to be incorporated into Green's function.

b) Sampling Green's Function by Random Walks

The development of the preceding section rests upon a crucial technical assertion, that it is possible to sample $(E_t + V_0)G(\underline{R},\underline{R}')$ or $(E_t + V_0)\psi_T(R)G(\underline{R},\underline{R}')/\psi_T(\underline{R}')$ for $\underline{R}$ conditional on $\underline{R}'$. Now for some simple problems - e.g., a particle in a box - one can construct the analytic form of G and hence an algorithm for sampling it. For interesting problems of statistical physics this is not possible, but we now sketch how it is possible to sample $G(\underline{R},\underline{R}')$ without knowing it explicitly. This algorithm is, of course, the heart of the method.

Let D be the full domain in configuration space in which the particles move. Consider some $D_0(\underline{R}_0) \subset D$ and suppose that

$$U_0 \geq V(\underline{R}) + V_0 \quad \text{for} \quad \underline{R} \in D_0 \quad . \tag{4.76}$$

We introduce the Green's function on the domain D_0, a "partial" Green's function

$$(-\nabla^2 + U_0)G_U(\underline{R}_1,\underline{R}_0) = \delta(\underline{R}_1 - \underline{R}_0) \quad \text{for} \quad \underline{R}_1,\underline{R}_0 \notin D_0 \tag{4.77}$$

with the boundary condition

$$G_U(\underline{R}_1,\underline{R}_0) = 0 \quad \text{for} \quad R_1,R_0 \notin D_0 \quad . \tag{4.78}$$

In principle U_0 could be a function of $\underline{R}$, but in practice only constant values have been used. The Green's functions introduced here are symmetric because of the boundary conditions. Equation (4.62) can be rewritten for a source at $\underline{R}_1$ as

$$[-\nabla_1^2 + V(\underline{R}_1) + V_0]G(\underline{R},\underline{R}_1) = \delta(\underline{R} - \underline{R}_1) \quad . \tag{4.79}$$

On multiplying (4.77) by $G(\underline{R},\underline{R}_1)$, (4.79) by $G_U(\underline{R}_1,\underline{R}_0)$, subtracting and integrating, one finds

$$\begin{aligned} G(\underline{R},\underline{R}_0) = G_U(\underline{R},\underline{R}_0) &+ \int_{\partial D_0(\underline{R}_0)} [-\nabla_{n_1} G_U(\underline{R}_1,\underline{R}_0)]G(\underline{R},\underline{R}_1)d\underline{R}_1 \\ &+ \int_{D_0(\underline{R}_0)} \{[U_0 - V(\underline{R}_1) - V_0]/U_0\}U_0 G_U(\underline{R}_1,\underline{R}_0)G(\underline{R},\underline{R}_1)d\underline{R}_1 \end{aligned} \quad . \tag{4.80}$$

This last equation shows how the full Green's function is related to a "partial" Green's function satisfying (4.76-78) on a subdomain. This relation may be understood in the following way. First observe that if (4.77) is integrated over $D_0(\underline{R}_0)$, we have

$$\int_{\partial D_0(\underline{R}_0)} [-\nabla_n, G_U(\underline{R}', \underline{R}_0)] d\underline{R}' + U_0 \int_{D_0(R_0)} G_U(\underline{R}', \underline{R}_0) d\underline{R}' = 1 \quad . \tag{4.81}$$

Since $G_U(\underline{R}, \underline{R}_0)$ and therefore $-\nabla_n, G_U(\underline{R}', \underline{R}_0)$ are non-negative, they may be interpreted as probability density functions for a move in a random walk which may go either to some $R' \in D_0(\underline{R}_0)$ or to $\underline{R}' \in \partial D_0(\underline{R}_0)$, respectively. Equation (4.80) may be related to expectations of random processes of this kind. In particular it expresses the fact that $G(\underline{R}, \underline{R}_0)$ is the sum of $G_U(\underline{R}, \underline{R}_0)$ for the subdomain plus the expected value of $G(\underline{R}, \underline{R}_1)$ taken over an ensemble of random events. These events comprise one of the following two possibilities: I) a move at random with density $-\nabla_{n_1} G_U(\underline{R}_1, \underline{R}_0)$ to $\underline{R}_1$ on the boundary $\partial D_0(\underline{R}_0)$; or II) a move at random with density $U_0 G(\underline{R}_1, \underline{R}_0)$ to $\underline{R}_1$ on the interior of $D_0(\underline{R}_0)$ with the averaging of $G(\underline{R}, \underline{R}_1)$ carried out with probability $[U_0 - V(\underline{R}_1) - V_0]/U_0$. It is true that in either case $G(\underline{R}, \underline{R}_1)$ is not known but we may now construct a domain $D_0(\underline{R}_1)$ containing $\underline{R}_1$. Then $G(\underline{R}, \underline{R}_1)$ may be expressed as in (4.80) as the sum of $G_U(\underline{R}, \underline{R}_1)$ plus the average of $G(\underline{R}, \underline{R}_2)$ taken over points $\underline{R}_2$ reached by random steps to the boundary or interior of $D_0(\underline{R}_1)$. The process may be iterated leading to a sequence of $\underline{R}_n$ with each chosen from its predecessor $\underline{R}_{n-1}$ by a move to $\underline{R}_n$ on the boundary of $D_0(\underline{R}_{n-1})$ drawn from $-\nabla_n G_U(\underline{R}_n, \underline{R}_{n-1})$ or to $\underline{R}_n$ on the interior of $D_0(\underline{R}_{n-1})$ drawn from $G(\underline{R}_n, \underline{R}_{n-1})$ and propagated with probability $[U_0 - V(\underline{R}_n) - V_0]/U_0$. $G(\underline{R}, \underline{R}_0)$ is the expected value of the sum of all the $G_U(\underline{R}, \underline{R}_n)$ for the $\underline{R}_n$ that are generated in this random walk. Each of these terms potentially makes a contribution to the next "generation" as in (4.64). That this procedure yields $G(\underline{R}, \underline{R}_0)$ can be proved formally, but we justify it here by a "physical" argument. Equation (4.62) has as its solution the expected density for observing at $\underline{R}$ an object which was started at $\underline{R}_0$ and which diffuses subject to an absorption process whose rate is $V + V_0$. Now at any stage of the diffusion process a domain $D_0(R) \subset D$ can be constructed. Green's function defined in (4.77,78) describes a diffusion in $D_0(\underline{R})$ subject to an absorption rate that is too large in the domain - cf. (4.76) - and to perfect absorption at the boundary. Diffusion continues until the first passage across that boundary. To describe the diffusion in the full domain such a first passage merely defines a surface source for subsequent diffusion. In addition the excess absorption owing to U_0 is compensated by the reintroduction of a fraction $\{[U_0 - V(R) - V_0]/U_0\}$ of those objects absorbed in the interior.

The details of the construction of the $D_0(\underline{R}')$ and the estimation of the upper bound $U_0(\underline{R}')$ are rather technical and depend upon the problem at hand. It has been found useful to construct $D_0(\underline{R})$ as a cartesian product of subspaces, one for each particle. Taking each subspace to be a sphere is especially convenient. Then separation of variables permits the explicit calculation of G_U as a product and this, in turn, leads to an explicit algorithm for sampling G_U.

The treatment of [4.28] does not include the absorption U_0, but the generalization is trivial. Let

$$(-\nabla^2 + \frac{\partial}{\partial t})G_0(\underline{R},\underline{R}',t) = \delta(\underline{R} - \underline{R}')$$

$$(-\nabla^2 + U_0 + \frac{\partial}{\partial t})G_U(\underline{R},\underline{R}',t) = \delta(\underline{R} - \underline{R}') \qquad (4.82)$$

with G_0 and G_U vanishing outside $D(\underline{R}')$ as before. Then

$$G_U(\underline{R},\underline{R}') = \int_0^\infty G_U(\underline{R},\underline{R}',t)dt = \int_0^\infty \exp(-U_0 t)G_0(\underline{R},\underline{R}',t)dt \quad . \qquad (4.83)$$

By sampling t from $U_0 \exp(-U_0 t)$ as well as the times described (3.11) in [4.28] the sampling of G_U is accomplished.

c) Importance Sampling

The sampling algorithm embodied in (4.80) yields a population drawn from $G(\underline{R},\underline{R}_0)$ for any $\underline{R}_0$. It must be altered to sample $\psi_T(\underline{R})G(\underline{R},\underline{R}_0)/\psi_T(\underline{R}_0)$ as indicated in (4.71). Again, formally this presents no particular problem. Equation (4.80) can be transformed by multiplying by $\psi_T(\underline{R})$ to produce

$$\begin{aligned}\psi_T(\underline{R})G(\underline{R},\underline{R}_0)/\psi_T(\underline{R}_0) &= \psi_T(\underline{R})G_U(\underline{R},\underline{R}_0)/\psi_T(\underline{R}_0) \\ &+ \int_{\partial D_0} [-\psi_T(\underline{R}_1)G_U(\underline{R}_1,\underline{R}_0)/\psi_T(\underline{R}_0)]\psi_T(\underline{R})G(\underline{R},\underline{R}_1)/\psi_T(\underline{R}_1)d\underline{R}_1 \\ &+ \int_{D_0} \{1-[V(\underline{R}_1) + V_0]/U_0\}U_0\psi_T(\underline{R}_1)G_U(\underline{R}_1,\underline{R}_0)/\psi_T(\underline{R}_0) \\ &\times \psi_T(\underline{R})G(\underline{R},\underline{R}_1)/\psi_T(\underline{R}_1)d\underline{R}_1 \qquad (4.84)\end{aligned}$$

to produce an integral equation for $\psi_T(\underline{R})G(\underline{R},\underline{R}_0)/\psi_T(\underline{R}_0)$. The new equation can also be sampled by a random walk in which the kernels which describe the passage from $\underline{R}'$ to $\underline{R}$ are modified by factors $\psi_T(\underline{R}')/\psi_T(\underline{R})$ - cf. the discussion following (4.80). We now show that the use of ψ_T is of very great potential in increasing the efficiency of the method.

To see how this may be possible, we define $E_T(\underline{R})$ by

$$(-\nabla^2 + V + V_0)\psi_T(\underline{R}) = [E_T(\underline{R}) + V_0]\psi_T(\underline{R}) \quad . \qquad (4.85)$$

Combining this with (4.77) which defines Green's function G_U, we obtain

$$\int_{aD_0(\underline{R}_0)} \{\psi_T(\underline{R}')[-\nabla_n G_U(\underline{R}',\underline{R}_0)]/\psi_T(\underline{R}_0)\}d\underline{R}'$$

$$+ \int_{D_0(\underline{R}_0)} \{[U_0 - V(\underline{R}') - V_0]\psi_T(\underline{R}')G_U(\underline{R}',\underline{R}_0)/\psi_T(\underline{R}_0)\}d\underline{R}' \quad . \tag{4.86}$$

$$= 1 - \int_{D_0(\underline{R}_0)} \{[E_T(\underline{R}') + V_0]\psi_T(\underline{R}')G_U(\underline{R}',\underline{R}_0)/\psi_T(\underline{R}_0)\}d\underline{R}'$$

Comparing with (4.80) we see that the first integral on the left is the expected number of steps to the boundary of $D_0(\underline{R}_0)$ which will be made when such steps are generated with density $\psi_T(\underline{R}')[-\nabla_n G_U(\underline{R}',\underline{R}_0)]/\psi_T(\underline{R}_0)$ in a random walk which generates $\psi_T(\underline{R})G(\underline{R},\underline{R}_0)/\psi_T(\underline{R}_0)$. The second integral on the left gives the expected number of corresponding steps to the interior of $D_0(\underline{R}_0)$.

When $E_T(\underline{R}) + V_0 \geq 0$ (a weak condition since $V(\underline{R}) \geq V_0$), the right side cannot exceed one. Thus the expected number of steps to boundary or interior of $D_0(\underline{R}_0)$ made in the Green's function random walk is generally less than one and the random walk terminates at some stage.

Now we recall that the n^{th} step in the random walk makes a contribution of $\psi_T(\underline{R})G_U(\underline{R},\underline{R}_n)/\psi_T(\underline{R}_n)$ to the full weighted Green's function $\psi_T(\underline{R})G(\underline{R},\underline{R}_0)/\psi_T(\underline{R}_0)$ and that each such partial contribution potentially contributes to the next generation of configurations. If $E_T(\underline{R})$ is replaced by E_t, then the integral on the right side of (4.86) is exactly the expected number of configurations in the next generation which results from the contribution of $G_U(\underline{R},\underline{R}_0)$ for domain $D_0(\underline{R}_0)$ to the full $G(\underline{R},\underline{R}_0)$. Now if ψ_T were ψ_0, the lowest eigenfunction, then $E_T = E_0 > V_0$, and we have the result that three possible events have probabilities that add up to one; the events are a move to the boundary, a move to the interior so as to continue the Green's function random walk, and the event that produces a configuration in the next generation. All three may then be sampled as mutually exclusive and exhaustive events. Thus one may arrange the algorithm so that the random walk terminates when and only when a next generation configuration is produced. Under these circumstances, viz., $\psi_T = \psi_0$ and $E_t = E_0$, the random walk produces exactly one new configuration and is guaranteed to terminate.

In addition, if (4.85) is combined with (4.62) defining the full Green's function, and the periodic and any other boundary conditions for ψ_T are used, the result is

$$\int \{[E_T(\underline{R}) + V_0]\psi_T(\underline{R})G(\underline{R},\underline{R}_0)/\psi_T(\underline{R}_0)\}d\underline{R} = 1 \quad . \tag{4.87}$$

Again, if $\psi_T(\underline{R}) = \psi_0(\underline{R})$ and $E_T(\underline{R}) = E_0$,

$$\left|\int [\psi_0(\underline{R})G(\underline{R},\underline{R}_0)/\psi_0(\underline{R}_0)]d\underline{R}\right|^{-1} = E_0 + V_0 \quad . \tag{4.88}$$

The integral on the left in (4.88) is simply the expected size of the total population, say N_2, which results in the next generation after one configuration at $\underline{R}_0(N_1 = 1)$ as in (4.68). With $E_t + V_0 = 1$ in (4.68) we see that the energy estimate from growth of generations is identically E_0, independent of $\underline{R}_0$ or any distribution used in sampling $\underline{R}_0$. The estimate of E then has zero variance, as does (4.69). Of course this ideal result requires knowing ψ_0, but we expect that "reasonable" ψ_T, such as those which prove useful in variational calculations will reduce the variance significantly. Much experience has borne this out although it is not necessarily true that the ψ_T in some class of trial functions which minimizes the energy also minimizes the variance. An important example will be discussed below.

d) Quantum Mechanical Expectations

In the preceding sections we have shown how the energy of the ground state can be estimated efficiently. But other expectations are also of considerable interest. These have the form

$$\langle F \rangle = \frac{\int \psi^*(\underline{R}) F \psi(\underline{R}) d\underline{R}}{\int |\psi(\underline{R})|^2 d\underline{R}} \tag{4.89}$$

$$= \frac{\int \psi_T \psi f(\underline{R}) \psi/\psi_T d\underline{R}}{\int (\psi_T \psi)(\psi/\psi_T) d\underline{R}} \quad . \tag{4.90}$$

The second of these assumes a real eigenfunction, that F is merely multiplication by $f(\underline{R})$ over some domain and casts the result in the form suitable for evaluation by Monte Carlo given a population of configurations drawn from $\psi_T(\underline{R})\psi(\underline{R})$. The extra factor or "weight" $\psi(\underline{R})/\psi_T(\underline{R})$ must be included. Now the completeness of the eigenfunctions of the hamiltonian implies

$$\sum_k \psi_T(\underline{R})\psi_k(\underline{R})\psi_T^{-1}(\underline{R}')\psi_k(\underline{R}') = \delta(\underline{R} - \underline{R}') \quad . \tag{4.91}$$

If one uses $\delta(\underline{R} - \underline{R}') = \psi_T(\underline{R})\psi^{(0)}(\underline{R})$ in the iteration (4.71) one sees easily [4.90] that the coefficient of the asymptotic value of $\psi_T\psi^{(n)}$ contains, aside from constants, the factors

$$\psi_T(\underline{R})\psi_0(\underline{R})\psi_T^{-1}(\underline{R}')\psi_0(\underline{R}')$$

so that the asymptotic generation size, conditional upon $\underline{R}'$, is $\psi_0(\underline{R}')/\psi_T(\underline{R}')$. Thus for each configuration, say $\underline{R}_k$, drawn from $\psi_T(\underline{R}_k)\psi(\underline{R}_k)$, further sampling can, in principle, yield statistically independent estimates of the weight to be given to $\underline{R}_k$.

Unfortunately, although importance sampling significantly accelerates this process, the computations have had to be carried to substantially greater length for reasonable estimates of quantities other than the energy by this method. That is, the variance of the weight is large for large numbers of generations.

If one assumes that $\psi_T(\underline{R})$ is close to $\psi_0(\underline{R})$, then a convenient estimate from a perturbation theory is possible. Let us define a "mixed expectation" as

$$\langle F\rangle_M = \frac{\int \psi_0\psi_T\cdot\psi_T^{-1}F\psi_T d\underline{R}}{\int \psi_T\psi_0 d\underline{R}} = \frac{\int \psi_0 F\psi_T d\underline{R}}{\int \psi_T\psi_0 d\underline{R}} \tag{4.92}$$

and write

$$\psi_0(\underline{R}) = \psi_T(\underline{R}) + \varepsilon\phi(\underline{R}) \tag{4.93}$$

$$\begin{aligned}\langle F\rangle_M &= \frac{\int \psi_T F\psi_T d\underline{R}}{\int \psi_T^2 d\underline{R}} + \frac{\varepsilon}{\int \psi_T^2 d\underline{R}}\left|\int \phi F\psi_T d\underline{R} - \frac{\int \phi\psi_T d\underline{R}\int \psi_T F\psi d\underline{R}}{\int \psi_T^2 d\underline{R}}\right| + O(\varepsilon^2)\\ &\equiv \langle F\rangle_T + \varepsilon F_1 + O(\varepsilon^2)\end{aligned} \tag{4.94}$$

where $\langle F\rangle_T$ is the purely variational estimate. A similar calculation yields for the true ground-state expectation

$$\langle F\rangle_0 = \langle F\rangle_T + 2\varepsilon F_1 + O(\varepsilon^2)$$

from which we derive an "extrapolated estimate"

$$\langle F\rangle_X = 2\langle F\rangle_M - \langle F\rangle_T = \langle F\rangle_0 + O(\varepsilon^2) \quad . \tag{4.95}$$

This method applies as well to the calculation of off-diagonal matrix elements (cf. Sect.4.4.1 below) and therefore to the treatment of condensate fractions and momentum distributions.

This estimate has been tested by comparing with values estimated from the asymptotic method, based on (4.91) and, more convincingly in certain cases, by carrying out calculations with different ψ_T and finding consistent extrapolated estimates

for expectations. Where the "extrapolated estimate" is unambiguous, it is preferable to the asymptotic results since it requires substantially less computation.

e) Implementation

The sampling of G_U [except for the extra step of sampling $U_0 \exp(-U_0 t)$] in cartesian product spaces is discussed in [4.28]. In particular it is shown that if each D_0 is taken as a product of one sphere for each coordinate then the algorithm reduces to the joint sampling of Green's functions for three dimensional spheres. The calculations of [4.28] were concerned with hard spheres only; the sphere radii were set simply by the condition that any pair of particles moving in or to the surfaces of their spheres could not approach closer than the hard-sphere diameter.

For calculations with a continuous potential, at least in part repulsive, the problem is somewhat more complicated. Although, in principle, any choice of domains $D_0(\underline{R})$ that can cover D may be used, the choice of size of domain and corresponding upper bound U_0 can strongly affect the efficiency. In treating potentials of the Yukawa type [4.59,91] the dominating factor is the r^{-1} singularity of the potential. There it was found reasonable to set $U_0 = \zeta V(\underline{R}_0)$ where ζ is a constant greater than one and to tabulate radii (as a function of nearest neighbor separation) such that moves in such spheres would not permit $V(R)$ to exceed U_0. Some experiments showed the computational efficiency not sensitive to ζ in the neighborhood of $\zeta = 2$.

In later computations of the Lennard-Jones potential, the method was somewhat more involved; U_0 was set to $V(\underline{R}_0) + V_1$, V_1 a constant determined from computer experiments. The average computing time required to sample completely a single iterate of the homogeneous (4.64) depends upon constants such as ζ and V_1 although average answers do not. These parameters may be varied in short auxiliary calculations to determine values which approximately minimize the computer time. In addition the value of V_0 was set to be about twice the minimum potential observed in practise, rather than a rigorous lower bound, with no complications arising.

Some discussion is worth giving here on the effect of the importance function upon the sampling of moves, that is, sampling $\psi_T(\underline{R})G_U(\underline{R},\underline{R}_0)/\psi_T(\underline{R}_0)$ rather than $G_U(\underline{R},\underline{R}_0)$. If one expands $\psi_T(\underline{R})$ about $\underline{R}_0$ through the first term, one has

$$\psi_T(\underline{R})/\psi_T(\underline{R}_0) = 1 + (\underline{R} - \underline{R}_0) \cdot \nabla\psi_T(\underline{R}_0)/\psi_T(\underline{R}_0) \quad . \tag{4.96}$$

The unmodified Green's function G_U is isotropic for each sphere. Thus the effect of (4.96) upon the marginal distribution of all variates except direction is nil. But the gradient of the log of ψ_T indicates a relative preference for some directions over others, e.g., a preference for a close pair to move apart.

In later evolutions of the method the practical effect of (4.86) on the sampling was recognized: for sampling steps which generate G from G_U, left side of (4.86),

the factor $[E_T(\underline{R}) + V_0]$ on the right acts as an effective "absorption" rate in decreasing the probability that the random walk continues when it is at $\underline{R}_0$.

Finally we note that the periodicity of the Green's function and of the wave function are ensured by the usual computational device [4.92] of moving by ± L any particle which leaves the domain at $\mp$ L/2. In this context this corresponds to using an infinite series of images (in the sense of potential theory) of the point $\underline{R}_0$.

We find that convergence to the ground state takes very roughly 50 generations starting from a population of configurations sampled from $|\psi_T(R)|^2$. The convergence does depend upon the accuracy of ψ_T to some extent and care must be taken to assure that convergence is complete. Indeed the principle complication and consumer of computer time is the necessity for computing accurate eigenvalues and expectations well beyond the point of apparent convergence to be sure of convergence to the required precision. With programs improved to the current state 64 body problems with Lennard-Jones forces require about 30 hours of time on a CDC 6600 to converge and give an average energy of better than 1%. For Yukawa forces the time is about a factor of 10 less.

4.4.1 Results

Early applications of the GFMC method included very simple few-body nuclear problems [4.93] and the helium atom [4.94]. A calculation [4.95] of 32 particles with Lennard-Jones forces of the de Boer-Michels type was somewhat more interesting. It used no importance sampling and was consequently very inefficient; it was the failure of that particular program to give anything reasonable for a system of 256 particles that gave the impetus to the development of importance sampling. But even with 32 particles, the result—later amply confirmed—that the energy of an ensemble of bosons with Lennard-Jones forces is substantially deeper than found variationally was first obtained.

In accord with the insightful suggestion of VERLET, the GFMC method was next applied to a hard-sphere quantum system, and the methodology considerably enhanced in the process.

The results [4.28] for the energy were somewhat (3-5%) deeper than found variationally, [4.40] and the radial distribution somewhat more structured. The improvement of agreement with experimentally measured structure functions was striking. Crystal calculations were made using ψ_T for the form given by (4.4). With the help of the perturbation theory also developed in [4.28], the energy for a Lennard-Jones system was estimated. A minimum of about -6.8 ± 0.2 K was obtained at a density of ρ = 1.0 ± 0.1 of the experimental density. The observed energy is -7.14 K.

The study of an inhomogeneous system of hard-sphere bosons was undertaken by LIU et al. [4.90]. Their system was periodic in two directions, but boundary conditions appropriate to hard parallel walls were applied in the third. This problem had also been studied using variational methods [4.42], where in the interior of the system a weakly layered density profile was found. These layers were strikingly enhanced in the GFMC results, as shown in Fig.4.3. In addition the interior structure was found to depend sensitively upon the width of the channel. New layers appear whenever the channel becomes wide enough to accommodate another peak of the ordinary radial distribution function. Interestingly the authors investigated a classical channel system at an appropriate density and found similar effects. PERCUS [4.95] was able to use a perturbation theory to relate quantitatively the channel results to the structure seen in a homogeneous system.

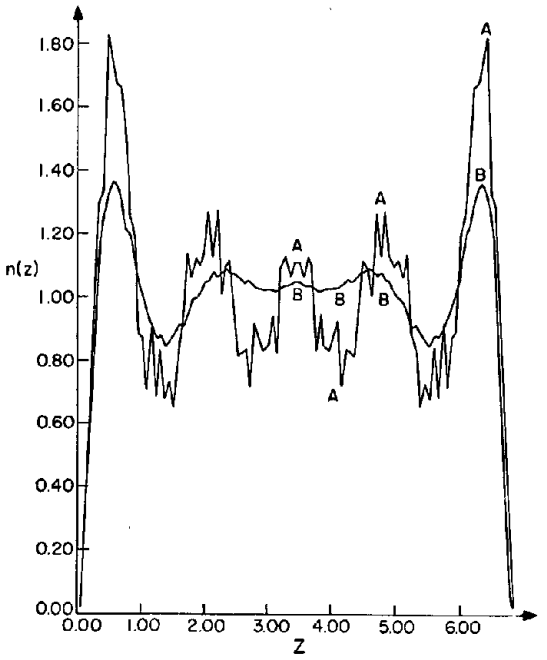

Fig.4.3 Density profiles for quantum hard spheres in a channel at average density $\rho a^3 = 0.2$. The width of the channel is 6.8a. The line B shows the results of a variational calculation, A the result of GFMC

LIU and KALOS [4.96] investigated the density profile of a film of bosons with two free surfaces using a hard-sphere plus square-well potential. This too showed fairly convincing evidence of layered structure near the surface. Unfortunately the model potential was not well suited for ^{4}He and the statistical errors in the density profile left something to be desired. This was a consequence mostly of the poor importance function ψ_T used to describe the homogeneous system.

Recently, WHITLOCK et al. [4.97] have returned to a direct calculation of ^{4}He with the de Boer-Michels form of the Lennard-Jones potential. This work is still in progress so only preliminary data are available. One important result is clear already: the potential used does indeed give a substantially deeper minimum than the variational results, confirming the previous results of KALOS [4.92] and of KALOS et al. [4.28], and in particular the perturbation theory of the latter paper. The newer results have much improved accuracy; a preliminary result for the equilibrium energy of liquid ^{4}He is -6.85 ± 0.05 K. This is uncorrected for three-body forces and correlations introduced by zero point motion of long wave-length phonons. These effects are being evaluated and appear to be about equal and of opposite sign.

The discrepancy in the energy as compared with the predictions of the product wave function (4.2) is even larger than one would expect from the error in the kinetic energy (as seen in the hard-sphere results) and the error amplifying effect of the cancellation by the negative potential energy. It seems likely that the neglect of three-body and higher correlations is the root of the problem [4.25].

The newer results on ^{4}He show again a more structured S(k) as compared with variational results – see Fig.4.4 – and reasonable agreement with recent experimental data for the momentum density in liquid ^{4}He obtained by MARTEL et al. [4.98] and by WOODS and SEARS [4.99]. The latter authors estimated the condensate fraction, n_0, at 1.1 K to be 6.9 ± 0.8% and extrapolated to 10.8 ± 1.3% at T = 0. The result obtained with GFMC [4.97] was 11.2 ± 0.2%. These are to be contrasted with the experimental results of 0.024 ± 0.01 and 0.018 ± 0.01 reported by MOOK et al. [4.100] and by MOOK [4.101], respectively.

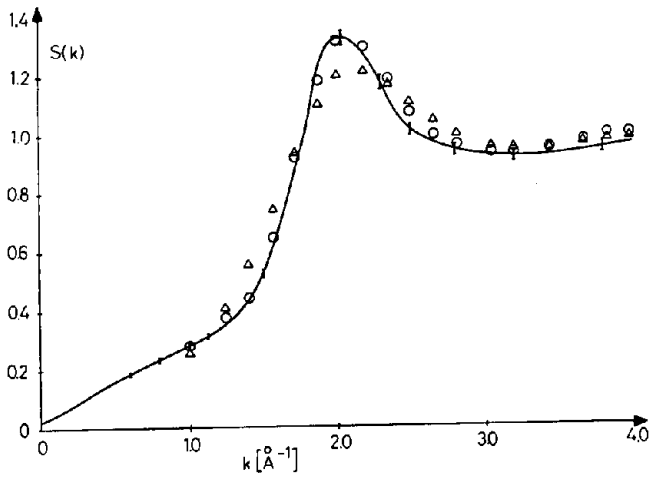

Fig.4.4 Comparison of structure functions for He-4 at equilibrium density. The solid line shows the smoothed experimental data of ACHTER and MEYERS [4.111] with bars indicating one standard deviation. S(k) computed variationally (Lennard-Jones 6-12; McMillan trial function) is shown by triangles. The circles show the results computed using GFMC

In the recent calculations of WHITLOCK et al. certain technical questions have been carefully investigated. In one case it was shown that the estimate of g(r) obtained from asymptotic weights [cf. discussion following (4.91)] is consistent with those obtained by extrapolation, (4.95). Also it was found that consistent energy values could be obtained when parameters of ψ_T were changed. Even more notable was a series of calculations at a density of $0.3648/(2.556\ \text{Å})^3$, the experimental equilibrium. At this density, product trial functions with pseudopotentials of very different character are available. GFMC calculations have been made with ψ_T having the McMillan form [4.1] and with the "α" and "β" functions suggested by de MICHELIS and REATTO [4.27]. It was found that use of the β function (constructed so as to agree well with experimental S(k) at the expense of a high energy value) reduced the variance of the energy estimates of the GFMC by a factor of 7 as compared with results obtained with McMillan's ψ_T. Thus the variational optimal is not necessarily the minimum variance ψ_T, although in no case was a ψ_T derived from variational results a poor choice. All three give consistent energy values. Most significant are that "extrapolated" estimates of g(r), S(k), <V> and n_0 (the condensate fraction) agree very well although the variational and "mixed" estimates, (4.94,92), respectively, are rather different. The validity of the extrapolation procedure is amply confirmed here.

CEPERLEY et al. have reported two investigations [4.59,91] on boson systems with Yukawa potentials. The variational calculations of these papers were described above in Sect.4.4. GFMC calculations were performed as well as a test of the accuracy of the energies and other quantities calculated. In general the variational energies are accurate; in the earlier paper [4.91] they are less than 1% above the GFMC results. Other expectations do not agree as well. The radial distribution is of the order of 10% more structured as calculated more exactly. In the second paper somewhat larger discrepancies were noted. One generally important point emerges from these results. Generally speaking, the energies deduced variationally for a crystal are more reliable than those found for the liquid, presumably owing to the simplification in the character of the wave function which results from crystal order. Thus the estimation of the location of melting and freezing transitions from variational energies is likely to be systematically biased.

In these papers also, additional verification of the independence of GFMC results to changes in ψ_T is given. In particular [4.59] compares calculations of energy with ψ_T of the gaussian type (4.34) or periodic (4.49). These give rather different variational energies but the GFMC results with the different ψ_T agree.

4.5 Virial Coefficients and Pair Correlations

FOSDICK and co-workers have published several papers [4.102-104] in which path integrals formulated to give the density matrix of a quantum system have been approximated by discrete paths and the resulting many dimensional integrals carried out by Monte Carlo. A review of the theory and an introduction to this class of approximations has been given also by BRUSH [4.105].

JORDAN and FOSDICK [4.102] calculated the second virial coefficient and pair correlation for a Lennard-Jones interaction. They regarded 2 K as a lower limit for the practical application of the method. Virial coefficients agreed within 2-3% of numerical values obtained from phase shifts. They calculated exchange contributions as well as direct, but at 2 K the exchange contribution to the pair correlation function showed very poor statistics.

In a second paper [4.103] the same authors included the effect of a third particle upon the pair correlations and estimated the third virial coefficient. This paper is technically interesting in that a version of the $M(RT)^2$ method [4.13] was used to sample paths representative of those required for the potential and the temperature involved. They reported results from 5 to 273 K but no permutation effects were included. The truncation errors (owing to replacement of continuous by straight paths) were made small compared to the Monte Carlo errors on say the pair distribution which ranged from a few to of the order of 20% in 20,000 samples. Interestingly, they found fair agreement with HENSHAW's data [4.106] for the pair distribution in liquid helium at 5 K.

Very recently WHITLOCK and KALOS [4.107] have taken up this class of problems, using the GFMC method to generate the quantum mechanical density matrix. They have formulated the general problem of treating a many-body system at finite temperature (including permutations to treat Bose or Fermi statistics) and treated in detail the pair correlation and second virial of a hard-sphere system. The general methods of Sect.4.4 above are followed except that an additional variable, the "pseudo time" = $1/k_BT$, is included in the full and partial Green's functions. An importance sampling transformation is introduced: there is an optimal importance function, namely the correct density matrix, which guides the random walk to the right place at the right "time". They found that approximate trial forms for the density matrix make the computation feasible but that improvements in that function improve the Monte Carlo efficiency in a drastic way. They were able to calculate direct and exchange pair correlations and virial coefficients from about 0.2 to about 10 K. The direct contributions were computed to about 7600 K. It is noteworthy that at high temperatures the difference between the quantum and classical pair correlations and virials is statistically significant. The worst error in the direct virial coefficients was obtained at low temperature—the standard error was 3% for 10^4 samples. The exchange virial grows worse at high temperatures and the best data at

8 K with the same number of samples give an error of 3%. All results were within statistical errors of those obtained by LARSEN [4.108] and by BOYD et al. [4.109] using partial wave expansions.

4.6 Conclusions

What, then, has been learned from these studies of quantum systems? First, it has been found that the product trial function is a good first approximation to the ground-state wave function of quantum liquids, and, with the gaussian localization, a good description of quantum solids. The variational method is able to predict qualitatively all of the zero temperature phase changes of helium and the quantitative energies are fairly close to the experimental values. The actual form of the pseudopotential is not very critical for computing ground-state energies but is important for other ground-state properties. The 'optimum' pseudopotential resulting from the 'paired-phonon' calculation of CHANG and CAMPBELL [4.25] is quite simple, consisting of the solution of the two-body Schrödinger equation for small r and the phonon pseudopotential of CHESTER and REATTO [4.9] for large r. The hypernetted chain integral equations are relatively accurate for quantum systems but are usually not reliable enough to predict phase transitions. In addition they are seriously inconsistent in estimating the kinetic energy.

The variational calculations have verified the intuitive picture of a crystal; the atoms move about the lattice sites with a gaussian density distribution. The ground-state energy is influenced very little by exchange effects.

Hence for most purposes one can regard the particles in crystals as distinguishable. The crystal becomes unstable if the rms displacement around a lattice site is greater than 0.27 of the nearest neighbor distance, this ratio depends only weakly on the interparticle potential and particle statistics.

There are many remaining unexplained problems for which quantum Monte Carlo is a powerful tool. First, it has been proposed [4.110] that all groups compute the equation of state of a more complicated neutron matter potential involving spin and tensor interactions. Monte Carlo can again provide a check on the various integral equation and cluster expansion techniques. Second, there are a number of interesting problems concerning quantum fluids and solids in restricted geometries which can be treated variationally as was done by LIU et al. [4.43,46]. Mixtures are also largely unexplored. Related to this are finite body problems such as nuclei, atoms, molecules and droplets which can in principle be approximated by product trial functions and for which Monte Carlo is particularly well suited since there are no periodic boundaries and hence no finite system size problems. The possibilities for the fermion Monte Carlo in molecular systems are interesting since it is radically different from present methods of calculation.

The variational method can be used to explore excited states. The product wave function in (4.3) is valid for excited states, where D is now an excited state of the ideal gas or harmonic crystal. The reweighting technique can be used to calculate accurately small differences between excited states.

Monte Carlo can also be used to explore a wider class of trial functions as was done by WOO and COLDWELL [4.38] for two-dimensional helium. FEYNMAN [4.83] has suggested a trial function incorporating back flow in Fermi liquids which is possible but perhaps tedious to sample with Monte Carlo.

The utility of GFMC is only now becoming apparent. It is true that it is not yet as convenient and economical a tool as variational studies. In careful studies of systems of ^{4}He such as the assessment of the effect of different potentials on the equation of state and other observable properties, it is likely to prove indispensable. In other research it should continue to be used to provide at the least critical "benchmarks" for the validity of less accurate methods.

As far as this review goes, the major lacuna is the absence of an exact numerical method, possibly of the GFMC type, for treating fermion systems. The fact that fermion wave functions have nodal surfaces whose character cannot usually be specified in advance is a major stumbling block but not necessarily an insuperable one.

We believe that the extension of GFMC to the treatment of equilibrium many-body problems at temperatures other than zero will be feasible and extremely useful. For the distant future the most remote speculations are for the development of a method capable of treating quantum many-body systems evolving in time.

Acknowledgements. We are grateful to K. BINDER, P.A. WHITLOCK, and G.V. CHESTER for helpful suggestions and critical review of the manuscript. The preparation of this review was begun while the authors were visiting the Laboratoire de Physique Théorique et Haute Energies at Orsay and they would like to thank B. JANCOVICI and D. LEVESQUE for their hospitality and the Centre National de la Recherche Scientifique for support. The work was also supported in part by the U.S. Department of Energy under contract. No. EY-76-C-02-3077.

References

4.1 W.L. McMillan: Phys. Rev. A *138*, 442 (1965)
4.2 D.C. Handscomb: Proc. Camb. Phil. Soc. *58*, 594 (1962); *60*, 115 (1964)
4.3 M. Suzuki, S. Miyashita, A. Kuroda, C. Kawabata: Phys. Lett. A *60*, 478 (1977)
M. Suzuki: Prog. Theor. Phys. *56*, 1454 (1976); Commun. Math. Phys. *51*, 182 (1976)
4.4 A. Bijl: Physica *7*, 869-886 (1940)
4.5 R.B. Dingle: Phil. Mag. *40*, 573 (1949)
4.6 R. Jastrow: Phys. Rev. *98*, 1479-1483 (1955)
4.7 N.F. Mott: Phil. Mag. *40*, 61 (1949)
4.8 E. Saunders: Phys. Rev. *126*, 1724-1736 (1962)
4.9 L. Reatto, G.V. Chester: Phys. Lett. *22*, 276 (1966)
4.10 R.P. Feynman: Phys. Rev. *94*, 262 (1954)

4.11 E. Krotscheck: Phys. Rev. A *15*, 397 (1977)
4.12 D. Bohm, D. Pines: Phys. Rev. *92*, 609 (1953)
4.13 N. Metropolis, A.W. Rosenbluth, M.N. Rosenbluth, A.M. Teller, E. Teller: J. Chem. Phys. *21*, 1087 (1953)
4.14 L. Verlet: Phys. Rev. *159*, 98 (1967)
4.15 J.D. Valleau, S.G. Whittington: "A Guide to Monte Carlo for Statistical Mechanics I", in *Modern Theoretical Chemistry*, Vol. V, Statistical Mechanics, ed. by B. Berne (Plenum Press, New York 1977)
4.16 D. Ceperley, G.V. Chester, M.H. Kalos: Phys. Rev. B *16*, 3081 (1977)
4.17 D. Ceperley: Monte Carlo study of the electron gas in two and three dimensions. Phys. Rev. B (in press)
4.18 S.G. Cochran: Ph. D. Thesis, Cornell University, Ithaca, New York (1973)
4.19 O. Penrose, L. Onsager: Phys. Rev. *104*, 576 (1956)
4.20 D. Levesque, Tu Khiet, D. Schiff, L. Verlet: Orsay report, 1965 (unpublished)
4.21 W.C. Stwalley, L.H. Nosanow: Phys. Rev. Lett. *36*, 910 (1976)
4.22 J. de Boer: Physica (Utrecht) *14*, 139 (1948)
4.23 D. Schiff, L. Verlet: Phys. Rev. *160*, 208 (1967)
4.24 R.D. Murphy, R.O. Watts: J. Low Temp. Phys. *2*, 507 (1970)
4.25 C.C. Chang, C.E. Campbell: Phys. Rev. B *15*, 4238 (1977)
4.26 J. Zwanziger: Ph. D. Thesis, Cornell University, Ithaca, New York (1972)
4.27 D. de Michelis, L. Reatto: Phys. Lett. A *50*, 275 (1974)
4.28 M.H. Kalos, D. Levesque, L. Verlet: Phys. Rev. A *9*, 2178 (1974)
4.29 R.D. Murphy: Phys. Rev. A *5*, 331 (1972)
4.30 J.P. Hansen, D. Levesque: Phys. Rev. *165*, 293 (1968)
4.31 J.P. Hansen: Phys. Lett. A *30*, 214 (1969)
4.32 J.P. Hansen, E.L. Pollack: Phys. Rev. A *5*, 2651 (1972); see also J.P. Hansen: J. Phys. C (Paris) *31*, Suppl. C *3*, 67 (1970)
4.33 R. Haberlandt: Phys. Lett. *14*, 197 (1965)
4.34 J.P. Hansen: Phys. Lett. A *34*, 25 (1971)
4.35 L.W. Bruch, I.J. McGee: J. Chem. Phys. *52*, 5884 (1970)
4.36 D.E. Beck: Mol. Phys. *14*, 311 (1969)
4.37 R.D. Murphy, I.J. McGee: Phys. Lett. A *45*, 323 (1973)
4.38 B.M. Axilrod, E. Teller: J. Chem. Phys. *11*, 293 (1943)
4.39 R.D. Murphy, J.A. Barker: Phys. Rev. A *3*, 1037 (1971)
4.40 J.P. Hansen, D. Levesque, D. Schiff: Phys. Rev. A *3*, 776 (1971)
4.41 J.D. Weeks, D. Chandler, H.C. Anderson: J. Chem. Phys. *54*, 5237 (1971)
4.42 K.S. Liu, M.H. Kalos, G.V. Chester: J. Low Temp. Phys. *13*, 227 (1973)
4.43 K.S. Liu, M.H. Kalos, G.V. Chester: Phys. Rev. B *12*, 1715 (1975); see also erratum, Phys. Rev. B
4.44 D.S. Hyman: Ph. D. Thesis, Cornell University, Ithaca, New York (1970) unpublished
4.45 C.E. Campbell, M. Schick: Phys. Rev. A *3*, 691 (1971)
4.46 K.S. Liu, M.H. Kalos, G.V. Chester: Phys. Rev. B *13*, 1971 (1976)
4.47 C.W. Woo, R.L. Coldwell: Phys. Rev. Lett. *29*, 1062 (1972)
4.48 C.E. Campbell: Phys. Lett. A *44*, 471 (1973)
4.49 J.V. Dugan, Jr., R.D. Etters: J. Chem. Phys. *59*, 6171 (1973)
R.D. Etters, J.V. Dugan, R.W. Palmer: J. Chem. Phys. *62*, 313 (1975)
4.50 R.L. Danilowicz, J.V. Dugan, Jr., R.D. Etters: J. Chem. Phys. *65*, 498 (1976)
4.51 M.D. Miller, L.H. Nosanow: Phys. Rev. B *15*, 4376 (1977)
4.52 L.H. Nosanow, L.J. Parish, E.J. Pinski: Phys. Rev. B *11*, 191 (1975)
M.D. Miller, L.H. Nosanow, L.J. Parish: Phys. Rev. Lett. *35*, 581 (1975)
M.D. Miller, L.H. Nosanow, L.J. Parish: Phys. Rev. B *15*, 214 (1977)
L.H. Nosanow: J. Low Temp. Phys. *26*, 613 (1977)
4.53 J.P. Hansen: Phys. Rev. *172*, 919 (1968)
4.54 T.A. Bruce: Phys. Rev. B *5*, 4170 (1972)
4.55 T.R. Koehler: Meth. Comp. Phys. *15*, 277 (1976)
4.56 G. Baym, C. Pethick: Ann. Rev. Nucl. Sci. *25*, 27 (1975)
4.57 S.G. Cochran, G.V. Chester: Preprint, Cornell University, Ithaca, New York (1973)
4.58 V.G. Pandharipande: Nucl. Phys. A *248*, 524 (1975)
4.59 D. Ceperley, G.V. Chester, M.H. Kalos: Phys. Rev. B *17*, 1070 (1978)

4.60 D. Schiff: Nat. Phys. Sci. *245*, 130 (1973)
4.61 R.G. Palmer, P.W. Anderson: Phys. Rev. D *9*, 3281 (1974)
4.62 J.P. Hansen, B. Jancovici, D. Schiff: Phys. Rev. Lett. *29*, 991 (1972)
4.63 R. Monnier: Phys. Rev. A *6*, 393 (1972)
4.64 H.R. Glyde, G.H. Keech, R. Mazighi, J.P. Hansen: Phys. Lett. A *58*, 226 (1976)
4.65 J.P. Hansen, R. Mazighi: Phys. Rev. A, to be published
4.66 L.L. Foldy: Phys. Rev. *124*, 649 (1961); *125*, 2208 (1962)
4.67 W.J. Carr: Phys. Rev. *122*, 1437 (1961)
4.68 F.Y. Wu, E. Feenberg: Phys. Rev. *128*, 943 (1962)
4.69 L.H. Nosanow, L.J. Parish: Ann. Acad. Sci. N.Y. *224*, 226 (1973)
4.70 J.P. Hansen, D. Schiff: Phys. Rev. Lett. *23*, 1488 (1969)
4.71 D.K. Lee, F.H. Ree: Phys. Rev. A *6*, 1218 (1972)
V.R. Pandharipande, H.A. Bethe: Phys. Rev. C *7*, 1312 (1973)
4.72 T. Gaskell: Proc. Phys. Soc. London *77*, 1182 (1961)
4.73 J.G. Zabolitzky: Phys. Rev. A *16*, 1258 (1977)
4.74 B. Day: Nuclear matter calculations. Rev. Mod. Phys. *50*, 495 (1978)
4.75 E.P. Wigner: Phys. Rev. *46*, 1002 (1934); Trans. Faraday Soc. *34*, 678 (1938)
4.76 C.M. Care, N.H. March: Advan. Phys. *24*, 101 (1975)
4.78 F.A. Stevens, Jr., M.A. Pokrant: Phys. Rev. A *8*, 990 (1973)
K.S. Singwi, A. Sjolander, M.P. Tosi, R.H. Land: Phys. Rev. B *1*, 1044 (1970)
D.L. Freeman: Phys. Rev. B *15*, 5512 (1977)
4.77 M. Cole: Rev. Mod. Phys. *46*, 451 (1974)
4.79 F. Bloch: Z. Physik (Leipzig) *57*, 549 (1929)
4.80 S. Mizawa: Phys. Rev. *140*, 1645 (1965)
4.81 A.K. Rajagopal, J.C. Kimball: Phys. Rev. B *15*, 2819 (1977)
4.82 T. Padmore, G.V. Chester: Phys. Rev. A *9*, 1725 (1974)
T.C. Padmore: Phys. Rev. Lett. *32*, 826 (1974)
4.83 R.P. Feynman, M. Cohen: Phys. Rev. *102*, 1189 (1956)
4.84 W.M. Saslow: Phys. Rev. Lett. *36*, 1151 (1976)
4.85 A.J. Leggett: Phys. Rev. Lett. *25*, 1543 (1970)
4.86 G. Meissner, J.P. Hansen: Phys. Lett. A *304*, 61 (1969)
4.87 E. Wigner: Phys. Rev. *40*, 729 (1932)
4.88 J.P. Hansen, J.J. Weis: Phys. Rev. *188*, 314 (1969)
4.89 J.P. Hansen, I.R. McDonald: Theory of Simple Liquids (Academic Press, New York 1976) p. 200
4.90 K.S. Liu, M.H. Kalos, G.V. Chester: Phys. Rev. A *10*, 303 (1974)
4.91 D.M. Ceperley, G.V. Chester, M.H. Kalos: Phys. Rev. D *13*, 3208 (1976)
4.92 M.H. Kalos: Phys. Rev. A *2*, 250 (1970)
4.93 M.H. Kalos: Phys. Rev. *128*, 1791 (1962); Nucl. Phys. A *126*, 609 (1969)
4.94 M.H. Kalos: J. Comp. Phys. *1*, 127 (1966)
4.95 J.K. Percus: J. Stat. Phys. *15*, 423 (1976)
4.96 K.S. Liu, M.H, Kalos: Unpublished
4.97 P.A. Whitlock, D.M. Ceperley, G.V. Chester, M.H. Kalos: Submitted to Phys. Rev.
4.98 P. Martel, E.C. Svensson, A.D.B. Woods, V.F. Sears, R.A. Cowley: J. Low Temp. Phys. *23*, 285 (1977)
4.99 A.D.B. Woods, V.F. Sears: Phys. Rev. Lett. *39*, 415 (1977)
4.100 H.A. Mook, R. Scherm, M.K. Wilkinson: Phys. Rev. A *6*, 2268 (1972)
4.101 H.A. Mook: Phys. Rev. Lett. *32*, 1167 (1974)
4.102 H.F. Jordan, L.D. Fosdick: Phys. Rev. *143*, 58 (1966)
4.103 H.F. Jordan, L.D. Fosdick: Phys. Rev. *171*, 128 (1968)
4.104 L.D. Fosdick, R.C. Jacobson: J. Comp. Phys. *7*, 157 (1971)
4.105 S.G. Brush: Rev. Mod. Phys. *33*, 79 (1961)
4.106 P.G. Henshaw: Phys. Rev. *119*, 14 (1960)
4.107 P.A. Whitlock, M.H. Kalos: Submitted to J. Comp. Phys.
4.108 S.Y. Larsen: J. Chem. Phys. *48*, 1701 (1968)
4.109 M.E. Boyd, S.Y. Larsen, J.E. Kilpatrick: J. Chem. Phys. *45*, 499 (1966)
4.110 H.A. Bethe: Workshop on Condensed and Nuclear Matter, May 3-6, 1977, Urbana, Ill., USA
4.111 E.K. Achter, L. Meyers: Phys. Rev. *188*, 291 (1969)